Nitrogen uptake and nitrification in the subarctic North Atlantic Ocean

Xuefeng Peng[1,2*], Sarah Fawcett[1,3*], Nicolas van Oostende[1], Martin Wolf[4], Dario Marconi[1], Daniel Sigman[1], and Bess Ward[1]

[1]Department of Geosciences, Princeton University

[2]Current address: Department of Earth Science, University of California, Santa Barbara

[3]Current address: Department of Oceanography, University of Cape Town

[4]Department of Earth, Atmospheric and Environmental Sciences, Massachusetts Institute of Technology

*Corresponding authors: xpeng@ucsb.edu; sarah.fawcett@uct.ac.za

Key words: nitrogen uptake, nitrification, biological pump, f-ratio, subarctic North Atlantic

Abstract

Nitrification, the oxidation of ammonium to nitrite and then nitrate, is often discounted as a source of nitrate in euphotic zone waters due to photoinhibition of nitrifying microorganisms and/or competition for ammonium with phytoplankton. However, there have also been counterarguments that nitrification represents a significant "regenerated" nitrate source to phytoplankton, augmenting the "new" nitrate supplied via physical processes. If nitrification is an appreciable nitrate source in the euphotic zone, then the assumption of a balance between nitrate uptake and organic matter export will overestimate export production. We investigated the relative importance of nitrification and nitrate uptake in the subarctic North Atlantic in late spring and late summer. The rates and vertical distributions of primary production, nitrogen uptake, and ammonium and nitrite oxidation were determined through isotope tracer experiments and the distributions of the nitrogen and oxygen isotopes of nitrate. In surface waters, ammonium and nitrite oxidation rates were low, representing an average of 5.2% and 2.5% of total euphotic zone nitrate uptake, respectively. The nitrogen and oxygen isotopes of nitrate confirmed that nitrification was not significant within the euphotic zone. Comparison of the rates of nitrogen uptake and primary production showed that while springtime phytoplankton growth could be fully supported by new nitrate and recycled ammonium, up to 50% of summertime productivity was likely fueled by dissolved organic nitrogen (DON). Uptake of DON implies that the fraction of primary production exported from surface waters in the late summer was significantly lower than the measured nitrate and ammonium uptake rates suggest.

Introduction

The ocean's biological carbon (C) pump plays an important role in controlling the atmospheric concentration of carbon dioxide (CO_2) by exporting a portion of the organic matter produced in surface waters (i.e., primary production) into the thermocline and deep ocean. Over large enough regions and timescales, it is expected that this "export production" is equivalent to the rate of "new production", defined as the quantity of primary production fueled by allochthonous nutrients supplied to the euphotic zone (Dugdale and Goering 1967). Two major sources of nitrogen (N) that support new production are N deriving from dinitrogen (N_2) fixation and subsurface nitrate (NO_3^-) supplied from below the euphotic zone via physical processes. The fraction of total primary production that is not "new" is termed "regenerated production" and is characterized as phytoplankton growth fueled by autochthonous nutrients produced by the remineralization of organic matter and/or zooplankton metabolism within the euphotic zone. Regenerated N is generally in the form of ammonium (NH_4^+) and dissolved organic N (DON) compounds such as urea (Bronk and Steinberg 2008). At an ecosystem level, the ratio of new production to total primary production (i.e., the "f-ratio", shorthand for "flux ratio"; Eppley and Peterson 1979) provides a measure of the strength of the biological pump, with a higher f-ratio indicating a greater proportion of carbon export relative to total carbon fixation. Since Dugdale and Goering (1967) first defined new production as the rate of NO_3^- uptake by phytoplankton in the euphotic zone, the f-ratio has been approximated by the ratio of NO_3^- uptake relative to NO_3^- plus NH_4^+ uptake (Eppley and Peterson 1979; Eqn. 1).

$$\text{f-ratio} = \frac{New\ Production}{New+Regenerated\ Production} = \frac{NO_3^-\ Uptake}{NO_3^-+NH_4^+\ Uptake} \quad \text{[Eqn. 1]}$$

The approach described above for evaluating the strength of the biological pump rests on the assumption that nitrification, the chemoautotrophic oxidation of NH_4^+ to nitrite (NO_2^-) and subsequently to NO_3^-, does not occur within the euphotic zone where it could represent a source of regenerated N. Historically, nitrification was largely neglected as a potential source of euphotic zone NO_3^- given the evidence for light inhibition of nitrifying microorganisms (Schön and Engel 1962; Hooper and Terry 1974; Horrigan et al. 1981; Olson 1981) and the fact that nitrifiers appear to be outcompeted by phytoplankton for NH_4^+ (Ward 1985, 2005; Smith et al. 2014). However, since the late 1980s, studies have shown that nitrification can sometimes constitute a significant source of NO_3^- in euphotic zone waters (Ward et al. 1989; Dore and Karl 1996; Martin and Pondaven 2006; Peng et al. 2016). If NO_3^- produced from nitrification (i.e., regenerated NO_3^-) is not accounted for in measurements of NO_3^- uptake,

both the f-ratio and the organic matter export flux will be overestimated. One modeling study has even argued that half of the NO_3^- consumed globally by phytoplankton is produced by euphotic zone nitrification, suggesting that NO_3^- uptake in surface waters is substantially higher than the amount of N exported from the euphotic zone (Yool et al. 2007). The authors compiled nitrification rate measurements from the open ocean, of which 64% derived from a location in the northeast Atlantic (Fernández 2003) where the average specific nitrification rates were about four times greater than all others in the dataset (Yool et al. 2007). In order to better understand the extent to which both regional f-ratios and the global ocean f-ratio may have been overestimated previously, it is necessary to evaluate the contribution of nitrification to NO_3^- uptake in the euphotic zone of oceanic regions that are poorly represented in the study by Yool et al. (2007).

The subarctic North Atlantic is one of the regions where direct rate measurements of nitrification are scarce, even though other major biogeochemical processes including primary, new, and regenerated production have been extensively investigated (e.g., Joint et al. 1993; Boyd et al. 1997; Bury et al. 2001; Bagniewski et al. 2011; Alkire et al. 2014; Van Oostende et al. 2017). As in other parts of the North Atlantic, productivity in most of the subarctic North Atlantic is limited by the availability of fixed N (Moore et al. 2013), and vertical mixing is considered the primary source of NO_3^- to euphotic zone waters. The region is characterized by some of the largest phytoplankton blooms on Earth, which begin in the spring as the mixed layer shoals and light levels rise. Rapidly growing diatoms typically dominate the spring bloom phytoplankton community, driving high rates of NO_3^- uptake and export production (Rynearson et al. 2013; Alkire et al. 2014; Cetinić et al. 2015). As silicate concentrations become limiting, diatom growth slows and smaller phytoplankton such as dinoflagellates and coccolithophores become dominant under the nutrient-deplete conditions characteristic of the late summer (Tarran et al. 2001; Dandonneau et al. 2004; Barton et al. 2013). Unsurprisingly, the f-ratio in the subarctic North Atlantic tends to be higher in the spring and early summer than later in the growing season (Bury et al., 2001 and references therein), although the potentially confounding effect of nitrification is not considered in the existing estimates.

Potentially overlapping N cycle processes, such as NO_3^- uptake and nitrification, can be tracked via natural variations in the N and oxygen (O) isotopes of NO_3^-. During NO_3^- uptake, the N and O isotopes are closely coupled, with phytoplankton preferentially consuming ^{14}N-

and ^{16}O-bearing NO_3^- such that the ambient NO_3^- pool becomes enriched in ^{15}N and ^{18}O as consumption proceeds (Granger et al. 2004, 2010; Rohde et al. 2015). In the upper water column, NO_3^- uptake by phytoplankton manifests as an equal rise in the $\delta^{15}N$ and $\delta^{18}O$ of NO_3^- (Trull et al. 2008; DiFiore et al. 2009; Rafter and Sigman 2016), concurrent with a decline in its concentration ($\delta^{15}N$, in ‰ vs. N_2 in air, = $\{[(^{15}N/^{14}N)_{sample}/(^{15}N/^{14}N)_{air}] - 1\}$ x 1000; $\delta^{18}O$, in ‰ vs. Vienna Standard Mean Ocean Water (VSMOW), = $\{[(^{18}O/^{16}O)_{sample}/(^{18}O/^{16}O)_{VSMOW}] - 1\}$ x 1000). By contrast, the production of NO_3^- via nitrification decouples the N and O isotopes of NO_3^- because the source of the N atoms incorporated into newly-nitrified NO_3^- is different from the source of the O atoms. The $\delta^{15}N$ of newly nitrified NO_3^- is controlled by the $\delta^{15}N$ of NH_4^+ being oxidized, which is set by the $\delta^{15}N$ of organic N undergoing remineralization (Sigman et al. 2005). Thus, from the perspective of the N atom in NO_3^-, nitrification and NO_3^- uptake are part of an internal cycle of fixed N that should cause no net change in NO_3^- $\delta^{15}N$ over time. On the other hand, nitrification is an absolute source of O atoms to NO_3^- and NO_3^- uptake is an absolute sink. Because >5/6 of the O atoms in NO_3^- originate from water, the $\delta^{18}O$ of newly-nitrified NO_3^- is largely set by the $\delta^{18}O$ of water (Sigman et al. 2009a; Buchwald et al. 2012) and does not depend on the source of the NH_4^+ being remineralized. The $\delta^{18}O$ of newly-nitrified NO_3^- has been estimated as 1.15‰ higher than ambient seawater based on ocean data (Sigman et al. 2009a), which appears consistent with the culture work to date (Buchwald et al. 2012). The difference between the N and O isotopes of NO_3^- with regard to remineralization/nitrification allows coupled N and O isotope measurements to separate processes that overprint one another (such as NO_3^- uptake and nitrification) when only NO_3^- $\delta^{15}N$ or $\delta^{18}O$ is considered (Sigman et al. 2005, 2009a,b; Wankel et al. 2007; Fawcett et al. 2015).

In order to understand the contribution of nitrification to new production in the subarctic North Atlantic Ocean, we conducted a series of onboard incubation experiments designed to yield rates of both N uptake (NO_3^- and NH_4^+) and nitrification, as well as C fixation (i.e., primary production), during late spring and late summer. Because these short-term incubations only provide snapshots of the N cycle processes that are active at the time of sampling, we also investigated the integrated signal of NO_3^- uptake and nitrification by measuring the N and O isotopes of NO_3^-.

Methods

Site description and physicochemical data collection

Samples for the incubation experiments and NO_3^- isotope measurements were collected in the subarctic North Atlantic during early autumn (September 2013; EN532) and late spring (May 2014; EN538) on board the R/V *Endeavor*. The locations of four process stations (PS) were selected (two in each season; Figure 1) to capture phytoplankton blooms based on sea surface chlorophyll data from satellite (NASA GSFC). Multiple conductivity, temperature, and depth (CTD) casts were deployed at each station to sample seawater for physicochemical measurements and incubation experiments. Nutrient samples were collected every 5-10 m over the upper 100 m and every 20-50 m between 100-1000 m. The depths from which seawater was collected for the incubation experiments were selected based on the physical structure of the water column (Table 1), which varied from day to day. Thus, even at the "same" station, features such as the mixed layer depth (MLD) and deep chlorophyll maximum depth varied over the time of our sampling.

At each station, light data from the daytime CTD casts were used to calculate the euphotic zone depth, which was defined as the depth at which photosynthetically active radiation (PAR) fell to 1% of its surface value (Kirk 1994). MLD was determined from vertical profiles of sigma-theta (σ_θ) calculated from temperature and salinity measured *in situ* during the CTD casts. The MLD criterion used was a threshold value of $\Delta\sigma_\theta = 0.03$ kg m^{-3} from the value at 10 m (de Boyer Montégut et al. 2004).

Nutrient concentrations were measured onboard according to the methods described in Van Oostende et al. (2017) and available at BCO-DMO #651816. In brief, seawater transferred from Niskin bottles into acid-washed HDPE bottles was handled using clean techniques to avoid contamination, following the international nutrient GO-SHIP manual (Hydes et al. 2010). For samples collected in September 2013, NH_4^+ was analyzed with an adapted fluorometric method, which uses a pH gradient to diffuse ammonia across a Teflon membrane prior to detection (Jones 1991). NO_3^- and NO_2^- were assayed using standard analytical methods adapted for low-concentration samples (Woodward and Rees 2001). The detection limit for NH_4^+ was 5 nmol l^{-1}, for NO_3^- was 1 nmol l^{-1}, and for NO_2^- was 0.5 nmol l^{-1}. For samples collected in May 2014, NH_4^+ was analyzed according to the fluorometric method of Holmes et al. (1999), with a detection limit of 15 nmol l^{-1}. NO_3^-+NO_2^- was determined by reduction to nitric oxide in a 95°C acidic vanadium (V(III)) solution followed

by nitric oxide analysis using a chemiluminescent detector (Teledyne model #200 EU) (Garside 1982; Braman and Hendrix 1989) in a configuration with a detection limit of 10 nmol l^{-1}. NO_2^- was measured according to the colorimetric method of Strickland and Parsons (1972) with a detection limit of 10 nmol l^{-1}, after which NO_3^--only concentrations were determined by subtraction from the chemiluminescence analyses of NO_3^-+NO_2^-.

Nitrogen and oxygen isotopes of nitrate and nitrite

Seawater samples for the analysis of the natural abundance N and oxygen (O) isotopes of NO_3^-+NO_2^- and NO_3^--only (see below) were collected unfiltered in acid-washed HDPE bottles and frozen at -20°C until analysis using the denitrifier method (Sigman et al. 2001; Casciotti et al. 2002; McIlvin and Casciotti 2011; Weigand et al. 2016). Briefly, sample NO_3^-+NO_2^- or NO_3^--only was quantitatively converted to nitrous oxide (N_2O) gas by *Pseudomonas aureofaciens*, a strain of denitrifying bacteria that lacks an N_2O reductase enzyme. The isotopic composition of the N_2O was then measured using a Thermo MAT 253 mass spectrometer with purpose-built on-line N_2O extraction and purification system. For quality control and calibration, seawater solutions of international NO_3^- reference materials, IAEA-N3 and USGS34, and an in-house N_2O standard were run in parallel with the samples. Using the configuration described above and the analysis approach outlined in Weigand et al. (2016), the standard deviation for repeat measurements is regularly better than 0.04-0.06‰ for $\delta^{15}N$ and 0.1-0.2‰ for $\delta^{18}O$.

If NO_2^- is present in seawater, even at very low concentrations, it can noticeably alter the N and O isotopic composition of NO_3^-+NO_2^- (Granger and Sigman 2009; Fawcett et al. 2015; Smart et al. 2015; Marconi et al. 2015). Calibrating measured O isotope ratios in seawater samples containing NO_2^- to NO_3^--only reference materials results in an underestimation of the $\delta^{18}O$ of the combined NO_3^-+NO_2^- pool (Casciotti and McIlvin 2007). We corrected the $\delta^{18}O$ of NO_3^-+NO_2^- for this methodological bias using the measured concentrations of NO_2^- and NO_3^-+NO_2^- and assuming a 25‰ difference between the $\delta^{18}O$ of N_2O produced by *P. aureofaciens* during the reduction of NO_3^- versus NO_2^- (Casciotti and McIlvin 2007; Fawcett et al. 2015). All NO_3^-+NO_2^- $\delta^{18}O$ data reported here have been corrected for this methodological bias.

To evaluate and remove the effect of ambient water column NO_2^- on the N and O isotopes of NO_3^-+NO_2^-, NO_2^- was removed from all samples collected above 500 m by adding 10 µl of

sulfamic acid solution (5% w/v in 10% hydrochloric acid) per ml of sample (Granger and Sigman 2009). The pH of the samples was restored to ~7-9 by the addition of 5.5 µl of 2M NaOH per ml of sample prior to analysis by the denitrifier method. For both NO_3^-+NO_2^- and NO_3^--only samples, the pooled standard deviation ($n \geq 3$) for $\delta^{15}N$ was 0.04‰ and for $\delta^{18}O$ was 0.14‰ for sample concentrations ≥ 0.5 µmol l^{-1}, and 0.11‰ and 0.25‰ for sample concentrations < 0.5 µmol l^{-1}.

The $\delta^{15}N$ of NO_2^- was calculated via isotope mass balance (Eqn. 2) using a Monte Carlo approach. The measured concentrations of NO_3^-+NO_2^- and NO_2^-, and the $\delta^{15}N$ of NO_3^-+NO_2^- and NO_3^--only were adjusted using random, normally distributed values and the measured standard deviations ($n \geq 3$) for each sample. NO_2^- $\delta^{15}N$ was then calculated 100,000 times using Eqn. 2. Here, we take the arithmetic mean and standard deviation of the 100,000 computations to be the best estimate of NO_2^- $\delta^{15}N$ and its associated uncertainty. Samples with NO_2^- concentrations less than 0.1 µmol l^{-1} were excluded from this analysis.

$$\delta^{15}N_{NO2} = ((\delta^{15}N_{NO3+NO2}*[NO_3^- + NO_2^-] - \delta^{15}N_{NO3}*([NO_3^- + NO_2^-] - [NO_2^-]))/[NO_2^-] \quad \text{[Eqn. 2]}$$

NO_3^- in the deep ocean is produced by nitrification, which uses ambient water as the dominant source of O atoms (Casciotti et al., 2002; 2010; Buchwald et al., 2012). Changes in the $\delta^{18}O$ of water will thus be reflected in the $\delta^{18}O$ of the produced NO_3^-. There exists a well-defined relationship between the $\delta^{18}O$ of seawater and its salinity (Craig and Gordon 1965), such that salinity-driven changes in ambient water $\delta^{18}O$ can drive changes in the $\delta^{18}O$ of NO_3^- (Knapp et al., 2008). To address this, we corrected NO_3^- $\delta^{18}O$ for the salinity-driven depth variations in seawater $\delta^{18}O$:

$$\delta^{18}O_{NO3(salinity\ corr)} = \delta^{18}O_{NO3} - (0.55 \times (sal - sal_{1000})) \quad \text{[Eqn. 3]}$$

where, $\delta^{18}O_{NO3}$ is the measured $\delta^{18}O$ of sample NO_3^-, 'sal' is the salinity of that sample as measured by the CTD, and 'sal_{1000}' is the mean salinity at 1000 m at each station. The factor of 0.55 is the approximate slope of the relationship between seawater $\delta^{18}O$ and salinity in the upper North Atlantic Ocean (LeGrande and Schmidt 2006). Correcting for changes in salinity decreased the $\delta^{18}O$ of NO_3^- in individual samples by a maximum of 0.23‰ in September (average of 0.15‰ at PS 1 and 0.11‰ at PS 2) and 0.15‰ in May (average of 0.11‰ at PS1 and 0.12‰ at PS2). All the NO_3^- (and NO_3^-+NO_2^-) $\delta^{18}O$ data presented here have been corrected this way.

Nitrogen isotopes of suspended particulate organic N (PON)

Suspended PON was collected from the surface to 100 m by gentle vacuum filtration (<135 mbar) of 4-8 L of seawater through a GF-75 filter (nominal pore size of 0.3 μm). In the laboratory, the PON filters were dried in a desiccating oven at 40°C. Three subsamples were cored from each filter and transferred to combusted 4 mL glass Wheaton vials. PON was oxidized to NO_3^- using the persulfate oxidation method of Knapp et al. (2005), as modified for samples on GF filters by Van Oostende et al. (2017); this reaction was conducted in a laminar flow hood equipped with an ammonia/amine filter to minimize contamination. The $\delta^{15}N$ of the oxidized NO_3^- was measured using the denitrifier method and corrected for the reagent+filter blank. The pooled standard deviation for corrected PON $\delta^{15}N$ ($n \geq 3$) was 0.16‰.

Nitrogen uptake and carbon fixation experiments and laboratory analyses

NH_4^+ and NO_3^- uptake and bicarbonate (HCO_3^-) fixation experiments were performed using seawater collected from three depths at each station (Table 1), with each depth being sampled on a separate day. The depths chosen correspond to light penetration levels of 30%, 2%, and 1% of surface PAR. At PS2 in May, experiments were also performed at a depth corresponding to 0.1% of surface PAR.

Seawater from the Niskin bottles was transferred into 4 L clear polycarbonate bottles and duplicate bottles were amended with 99 at-% $^{15}NH_4Cl$, $Na^{15}NO_3$, or $NaH^{13}CO_3$ to reach a ^{15}N-substrate addition of ~10% and a ^{13}C-substrate addition of ~5%. Prior to incubation, seawater from the same Niskin bottles was measured for NH_4^+ and NO_3^- concentrations in order to determine the appropriate level of tracer addition. Ambient dissolved inorganic carbon (DIC) concentrations were assumed to be 2100 μmol l^{-1} (Zunino et al., 2015). The polycarbonate bottles were incubated for six hours in running surface seawater incubators, and *in situ* light conditions were simulated using mesh screens. After incubation, the seawater in each bottle was filtered through a 47 mm diameter GF-75 filter that was stored frozen at -80°C until analysis.

In the laboratory, thawed filters were exposed to the fumes of concentrated hydrochloric acid for approximately 4 hours to remove inorganic carbon and then dried overnight in an oven at 60°C. After the excess rims of the filters were trimmed, they were sliced in half to produce

technical replicates, each of which was packaged into a tin capsule. Pelletized capsules were analysed using a Europa 20/20 elemental analyser-triple collector mass spectrometer for N and C content and isotopic composition. Sample measurements were corrected for the N and C blank, which consisted of a tin capsule containing a blank pre-combusted GF-75 section. Daily standard curves bracketing anticipated sample masses were run prior to the samples using urea as a laboratory standard; from these calibration curves, sample N and C content was calculated. The measured N and C isotopic composition was calibrated using peach leaf (NIST-1547) and L-glutamic acid (USGS-40; Qi et al. 2003) standards run in parallel with the samples. The standard errors of laboratory standards were 0.05 μmol N and 0.34‰ at 3.33 μmol N, and 0.14 μmol C and 0.07‰ at 6.66 μmol C.

The rates of NH_4^+ and NO_3^- uptake (ρ_{NH4} and ρ_{NO3}, respectively) were calculated as in Dugdale and Goering (1967) and Legendre and Gosselin (1997) with slight modifications (Supplementary Information S2). The initial ratio of $^{15}N/^{14}N$ in the dissolved inorganic nitrogen (DIN) pool was calculated from the measured ambient concentration of NH_4^+ or NO_3^-, the $\delta^{15}N$ of NH_4^+ or NO_3^-, and the concentration and $^{15}N/^{14}N$ (0.99) of the tracer addition. The $\delta^{15}N$ of ambient NH_4^+ was assumed to be 3‰ lower than the measured $\delta^{15}N$ of ambient PON (Altabet and Small 1990; Fawcett et al. 2011; Möbius 2013), while the $\delta^{15}N$ of ambient NO_3^- was measured using the denitrifier method (Sigman et al. 2001). ρ_{NH4} and ρ_{NO3} were converted to per day rates (i.e., nmol l^{-1} d^{-1}) assuming 12 hours of daylight. Finally, at each depth, the f-ratio was calculated according to Eppley and Peterson (1979) as:

$$f = \rho_{NO3}/(\rho_{NO3} + \rho_{NH4}) \qquad \text{[Eqn. 4]}$$

Below, we report and discuss only the euphotic zone average f-ratios for each station, calculated by trapezoidally integrating the f-ratios measured at each depth and then dividing by the depth of the euphotic zone (i.e., a weighted average).

The hourly rate of photosynthetic carbon fixation was determined by normalizing the rate of DIC incorporation into POC to the length of the incubation, calculated following Legendre and Gosselin (1997). The duration of the carbon fixation incubations (~7-9 hours, beginning at dawn) means that the resultant rates best approximate net primary production (NPP) (Cullen, 2001). Carbon fixation rates were converted to per day rates (i.e., nmol l^{-1} d^{-1}) assuming uptake occurred during the 12 hours of daylight.

Nitrification incubation experiments and laboratory analyses

Incubation experiments to measure NH_4^+ and NO_2^- oxidation rates were performed onboard with seawater collected from the depths indicated in Table 1. Approximately 450 ml of seawater was transferred directly from the Niskin bottles into tri-laminate opaque bags, and ^{15}N-labeled substrates were injected as the seawater was flowing into the bags to ensure complete mixing. $^{15}NH_4^+$ + $^{14}NO_2^-$ were added to the NH_4^+ oxidation incubations, and $^{15}NO_2^-$ was added to the NO_2^- oxidation incubations. The exact volume in each bag was measured using a 500-ml graduated cylinder at the end of incubation. The final concentrations of the $^{15}NH_4^+$ and $^{14}NO_2^-$ additions were ~0.02 μmol l^{-1}, and the final concentration of $^{15}NO_2^-$ was ~0.05 μmol l^{-1}. After 12 hours of incubation at near *in situ* temperatures, 45 ml of sample were collected in a 50 ml centrifuge tube and immediately frozen at -80°C.

The isotopic composition of NO_2^- in the samples from the NH_4^+ oxidation incubations was measured following the azide method of McIlvin and Altabet (2005), which converts NO_2^- into N_2O, with amendments as detailed in Peng et al. (2015). Briefly, helium-purged samples were incubated with azide reagents (1 mol l^{-1} sodium azide in 10% acetic acid) for 15 min in gas-tight vials, followed by the addition of 10 mol l^{-1} sodium hydroxide to raise the sample pH to > 12. The isotopic composition of N_2O was determined using a Delta V isotope ratio mass spectrometer coupled to a purge-and-trap front end. The detection limit was 0.2 nmol N, and the precision for $\delta^{15}N$ was 0.2‰ ($n \geq 3$).

The rate of NH_4^+ oxidation (V_{NH4}) was calculated from the equation:

$$V_{NH_4^+} = \frac{\Delta[^{15}NO_2^-]}{f^{15}_{NH_4^+} \times T} \qquad \text{[Eqn. 5]}$$

where $\Delta[^{15}NO_2^-]$ is the change in concentration of $^{15}NO_2^-$ between the start and the end of the incubation due to NH_4^+ oxidation (nmol l^{-1}), $f^{15}_{NH_4^+}$ is the fraction of NH_4^+ labeled with ^{15}N at the start of the incubation, and T is the length of incubation (days). For the September 2013 cruise, the concentration of $^{15}NO_2^-$ at the start of the incubation ($[^{15}NO_2^-]_0$) was calculated using the $\delta^{15}N$ of NO_2^- computed from measurements of the $\delta^{15}N$ of NO_3^-+NO_2^- and NO_3^--only samples (see above). For the May 2014 cruise, $[^{15}NO_2^-]_0$ was measured from samples

collected at the start of the incubation. The detection limit for the NH_4^+ oxidation experiments was determined foreach incubation following Santoro et al. (2013), and depends on the fraction of substrate labeled with ^{15}N at the beginning of the incubation and the concentration of the product pool. It ranged from 0.01 to 0.50 nmol l^{-1} d^{-1}, except at 100 m at PS1 in September (detection limit = 1.11 nmol l^{-1} d^{-1}) where the NH_4^+ concentration (2.64 µmol l^{-1}) was anomalously high.

The isotopic composition of NO_3^- in the samples from the NO_2^- oxidation incubations was measured using the denitrifier method (Sigman et al. 2001; McIlvin and Casciotti 2011). Since this method converts both NO_3^- and NO_2^- to N_2O, samples were first treated with 15 mmol l^{-1} sulfamic acid (final concentration) to remove any remaining NO_2^-, after which the pH was restored to ~7 with 2 mol l^{-1} NaOH (Granger and Sigman 2009). The efficiency of NO_2^- removal was >97.5%, and the trace amount of remaining contaminant $^{15}NO_2^-$ was accounted for as in Peng et al. (2015). Three international NO_3^- reference materials (IAEA-N3, USGS 34, and USGS 32) were used to calibrate the $\delta^{15}N$ of NO_3^-.

The rate of NO_2^- oxidation (V_{NO2}) was calculated from the equation:

$$V_{NO_2^-} = \frac{\Delta[^{15}NO_3^-]}{f^{15}_{NO_2^-} \times T} \qquad \text{[Eqn. 6]}$$

where $\Delta[^{15}NO_3^-]$ is the change in concentration of $^{15}NO_3^-$ between the start and the end of the incubation (nmol l^{-1}) due to NO_2^- oxidation, $f^{15}_{NO_2^-}$ is the fraction of NO_2^- labeled with ^{15}N at the start of the incubation, and T is the length of incubation (days). For the September 2013 cruise, the concentration of $^{15}NO_3^-$ at the start of the incubation ($[^{15}NO_3^-]_0$) was calculated from the measured $\delta^{15}N$ of NO_3^- for samples collected at the same station. For the May 2014 cruise, $[^{15}NO_3^-]_0$ was measured from samples collected at the start of the incubation. The detection limit (Santoro et al. 2013) for the NO_2^- oxidation experiments was 0.05-0.67 nmol l^{-1} d^{-1}. We did not account for possible isotope dilution due to regeneration of the ^{15}N-labeled N substrate, so the calculated NH_4^+ and NO_2^- oxidation rates may be underestimates.

The euphotic zone integrated rates of NH_4^+ and NO_3^- uptake (ρ_{NH4_integ} and ρ_{NO3_integ}) and NH_4^+ and NO_2^- oxidation (V_{NH4_integ} and V_{NO2_integ}) were calculated by trapezoidally integrating the incubation rates measured between the surface and the base of the euphotic

zone. Where no measurements were available for the base of the euphotic zone, rates were estimated by linear interpolation prior to integration.

Results

Hydrography

Surface NO_3^- concentrations ($[NO_3^-]$) in September 2013 were nearly zero, whereas in May 2014, surface $[NO_3^-]$ ranged from 5-8 μmol l^{-1} (Figure 1). Mixed layer depth (MLD) fluctuated considerably (by 15 m to 40 m) during the five to six days of process station occupation in both seasons (Figure 2). The depth of 1% PAR was deeper than the MLD on most days at all stations, with the exception of a few short episodes of MLD deepening at PS1 in September 2013 and PS2 in May 2014. In September 2013, the nitracline (determined after Van Oostende et al. (2017)) was deeper than the MLD, while in May 2014, the nitracline was not as pronounced and overlapped with the MLD (Figures 2 to 4). A subsurface maximum concentration of NH_4^+ (up to ~1 μmol l^{-1}) and NO_2^- (0.3-0.6 μmol l^{-1}) was observed at all stations except PS1 in May 2014. N uptake experiments were performed within the mixed layer, except for two experiments from depths below the MLD in May 2014 (Figure 2C, D). Nitrification incubation experiments were performed both within and below the mixed layer.

Nitrogen uptake and carbon fixation rates

In September, the NH_4^+ uptake rate (ρ_{NH4}) increased from the surface to the base of the euphotic zone at both stations, while the rate of NO_3^- uptake (ρ_{NO3}) decreased with depth (Figure 3). In May, the N uptake patterns were slightly different, with ρ_{NH4} and ρ_{NO3} showing similar changes with depth. At PS1, both ρ_{NH4} and ρ_{NO3} decreased from 25 m to 45 m, and then increased again at the base of the euphotic zone (Figure 4). The uptake rate measurements at 45 m coincided with a deepening of the MLD. At PS2, ρ_{NH4} and ρ_{NO3} decreased with depth, and were still detectable as deep as 82 m, well below the base of the euphotic zone (57 m), which was just below the MLD at this station (Figure 2D).

The rates of carbon fixation (i.e., NPP) decreased with depth in the water column, with the exception of PS1 in May where NPP was highest at the deepest sample depth (50 m; Figures 3 and 4). In addition, euphotic zone integrated rates of NPP were generally higher in September than in May (Table 2). While the highest rate of NO_3^- uptake occurred at the

station also characterized by the highest NPP (September PS 1), we observed no clear relationship between NPP and NO_3^- uptake.

The daily rates of NH_4^+ and NO_3^- uptake, integrated over the euphotic zone (ρ_{NH4_integ} and ρ_{NO3_integ}), are listed in Table 1. The combined rates of NH_4^+ and NO_3^- uptake were positively correlated with the euphotic zone integrated total particulate organic nitrogen (PON_{integ}; Pearson's correlation coefficient = 0.91, Figure S1). The average euphotic zone f-ratio coincided with euphotic zone integrated ρ_{NO3} in the sense that it was highest at PS1 (0.62) and lowest at PS2 (0.20) in September (Table 1). In May, the average euphotic zone f-ratio was similar for both stations, 0.39 and 0.40 for PS1 and PS2, respectively, and did not change (0.39) with a deeper integration depth at PS2 (i.e., 82 m rather than 57 m).

Nitrification Rates

Both the NH_4^+ and NO_2^- oxidation rates showed a subsurface maximum just below the euphotic zone in September and May (Figures 3 and 4). At three out of the four stations, the subsurface maximum NO_2^- oxidation rates occurred slightly deeper than their coincident NH_4^+ oxidation rate maxima. With a few exceptions in late summer, NO_2^- oxidation rates were generally lower than NH_4^+ oxidation rates. The depth of the subsurface maximum NH_4^+ oxidation rates was either the same or slightly greater (by 5-20 m) than the observed depth of the subsurface maxima in NH_4^+ concentration. The subsurface maximum in NO_2^- oxidation rates overlapped in depth with the NO_2^- concentration maximum (Figures 3 and 4).

Where measured at the same depths, NH_4^+ uptake rates were generally one to two orders of magnitude higher than NH_4^+ oxidation rates, except at 82 m (0.1% PAR) at PS2 in May 2014, where the NH_4^+ oxidation rate was roughly double the NH_4^+ uptake rate (Figure 4). Integrated over the euphotic zone, NH_4^+ oxidation constituted 1.04% (PS2 in May) to 10.9% (PS2 in September) of ρ_{NO3_integ} and NO_2^- oxidation constituted 0.36% (PS1 in September) to 5.14% (PS2 in September) of ρ_{NO3_integ}. Except at PS2 in May, V_{NH4_integ} was always greater than V_{NO2_integ} (by a factor of 2.1 to 5.1; Table 1); however, if the integration depth at PS2 in May is taken to be 82 m rather than 57 m, V_{NH4_integ} was 2.7 times greater than V_{NO2_integ}. Given the possibility of phytoplankton-nitrifier competition for NH_4^+ substrate (Ward 1985, 2005; Smith et al. 2014), we also calculated the euphotic zone integrated ratio of NH_4^+ uptake and NH_4^+ oxidation ($\rho_{NH4\_integ}/V_{NH4\_integ}$), which illustrates the capacity of autotrophs relative to NH_4^+ oxidizers to leverage the available NH_4^+ pool. This exercise shows that ρ_{NH4_integ} was

23 to 146 times greater than euphotic zone V_{NH4_integ}; this became 9.5 to 36 times if the integration depth for PS2 in May is increased to 82 m.

The N and O isotopes of nitrate and nitrite

The $\delta^{15}N$ of $NO_3^-+NO_2^-$ below 200 m was very similar at all four stations (average of 4.80 ± 0.02‰; Figure 5A, C). Above 200 m in September and 150 m in May, $NO_3^-+NO_2^-$ $\delta^{15}N$ increased into the surface layer. After NO_2^- removal, the $\delta^{15}N$ of NO_3^--only in the surface layer for all samples with $[NO_2^-] \geq 0.1$ μmol l^{-1} increased by 0.50‰ to 2.18‰ (average of 1.50 ± 0.64‰) in September and 0.18‰ to 0.97‰ (average of 0.46 ± 0.21‰) in May (Figure 5A, C). The more pronounced rise in September is due to NO_2^- constituting a greater fraction of the $NO_3^-+NO_2^-$ pool at this time (average of 5.6 ± 6.6% vs. 1.4 ± 0.7% in May; Figures 3, 4, and 6).

The average $\delta^{18}O$ of $NO_3^-+NO_2^-$ between 1000 m and 600 m at all stations was 1.82 ± 0.13‰, increasing gradually upward to 4.32 ± 0.26‰ at 100-200 m just below the euphotic zone (Figure 5B, D). Within the euphotic zone, variability among the profiles increased, but in all cases, $\delta^{18}O$ of $NO_3^-+NO_2^-$ increased considerably due to NO_3^- uptake by phytoplankton. The variability among profiles is more pronounced after NO_2^- removal, which increased NO_3^- $\delta^{18}O$ by an average of 2.05 ± 0.44‰ (range of 1.14‰ to 2.40‰) in September and 0.29 ± 0.23‰ (range of 0.02‰ to 0.86‰) in May.

The calculated NO_2^- $\delta^{15}N$ in the upper 200 m ranged from -11.1 ± 3.3‰ to -0.9 ± 1.2‰ in September and -36.9 ± 12.9‰ to -9.0 ± 5.2‰ in May (Figure 6B). The mass-weighted average NO_2^- $\delta^{15}N$ for all samples with NO_2^- concentrations ≥ 0.1 μmol l^{-1} was -8.0 ± 3.3‰ and -2.7 ± 1.1‰ for September PS1 and PS2, respectively, and -19.7 ± 8.6‰ and -31.6 ± 12.0‰ for May PS1 and PS2, respectively.

Discussion

The subarctic North Atlantic has been studied extensively for its high primary productivity and characteristic massive seasonal phytoplankton blooms (e.g., Joint et al. 1993; Boyd et al. 1997; Bury et al. 2001; Bagniewski et al. 2011; Alkire et al. 2014; Van Oostende et al. 2017). The high rates of export production directly measured in this region indicate a strong biological pump, high dependence on NO_3^-, and high f-ratios (Buesseler et al. 1992; Honjo

and Manganini 1993). However, f-ratios could be overestimated by neglecting the possibility of nitrification as a source of regenerated NO_3^- within the euphotic zone, as highlighted by a global meta-data study (Yool et al. 2007). We used a multi-faceted approach to evaluate the contribution of nitrification to the euphotic zone NO_3^- supply in the subarctic North Atlantic during the late summer (September 2013) and late spring (May 2014).

In September, the depleted surface NO_3^- concentrations (0.03-1.9 μmol l^{-1}) were typical for late summer in this region (World Ocean Atlas 2013, September; Garcia et al. (2013)) when the phytoplankton community was dominated by regenerated N specialists (i.e., picocyanobacteria and picoeukaryotes) (Van Oostende et al. 2017). In May, the relatively depressed euphotic zone chlorophyll concentrations (0.5-1.5 μg l^{-1}; Van Oostende et al., unpublished) indicate that we did not capture a phytoplankton bloom, and the high surface NO_3^- concentrations at this time (5-8 μmol l^{-1}) suggest that factors such as silicate or micronutrient availability combined with low light levels were limiting primary productivity (Martin-Jézéquel et al. 2000; Nielsdóttir et al. 2009). Below, we first discuss the N uptake and nitrification rates separately, and then evaluate the potential role of nitrification in supplying NO_3^- to phytoplankton in the euphotic zone of the subarctic North Atlantic. Finally, we address other potential biogeochemical processes that may complicate estimates of new, regenerated, and export production based on NO_3^- and NH_4^+ uptake. Our analysis suggests that uptake of dissolved organic nitrogen (DON) contributed significantly to regenerated production in late summer but not in late spring.

Uptake of nitrate and ammonium in the subarctic North Atlantic

Broadly, the euphotic zone integrated rates of NO_3^- and NH_4^+ uptake differed little between September and May; indeed, inter-station variability during the same season was generally greater than the seasonal differences (Table 1). This is consistent with the observation that total euphotic zone chlorophyll was similar in both seasons (39-48 mg m^{-2}), albeit slightly lower at PS2 in September, which, based on the nutrient concentration data, was the most oligotrophic station sampled (Van Oostende et al., 2017; Ward et al. 2016 dataset). Collectively, the rate data indicate that the May sampling did not capture a phytoplankton bloom as might have been expected in the spring. Integrated NO_3^- uptake rates of 18 mmol m^{-2} d^{-1} have been measured during the North Atlantic spring bloom in the vicinity of our study (Bury et al. 2001), while our rates were 0.8-3.6 mmol m^{-2} d^{-1} (Table 1).

There were, however, differences in the vertical distribution of NO_3^- and NH_4^+ uptake between seasons. In September, NO_3^- uptake rates were highest in the surface and decreased with depth, whereas NH_4^+ uptake increased with depth (Figure 3). Given that it is less energetically expensive to assimilate NH_4^+ than NO_3^- (Dortch 1990), this pattern may be explained by the vertical gradient in light availability through the upper water column. Near the surface where light levels are high, phytoplankton can easily acquire the reducing power needed to assimilate NO_3^-. However, under the low light conditions of the lower euphotic zone, this is more difficult, and phytoplankton increase their dependence on NH_4^+ despite the increase in NO_3^- concentration. It is also possible that the high NH_4^+ concentrations measured at the base of the euphotic zone in September rendered the uptake of this N source more favorable than it might otherwise have been.

In May, the vertical distribution of NH_4^+ and NO_3^- uptake at PS1 was variable (Figure 4), possibly due to the rapidly changing MLD (Figure 2C) driving variability in the light field experienced by phytoplankton. At PS2 by contrast, MLD was fairly constant over the experimental period (Figure 2D), and both NO_3^- and NH_4^+ uptake decreased with depth in the presence of non-limiting NO_3^- and NH_4^+ concentrations. This can also be attributed to light, as the deepest experiment at PS2 was conducted at the 0.1% light depth (82 m) where light availability likely limited both NO_3^- and NH_4^+ uptake (Thompson et al. 1989).

At the height of the North Atlantic spring bloom, f-ratios of 0.45-0.76 (48-50°N, 20°W; Bury et al., 2001) and 0.62-0.93 (62°N, 20°W; Boyd et al. 1997) have been measured in the Northeast Atlantic, indicating high dependence on NO_3^-. At the time of our September and May sampling, however, the upper ocean ecosystem was predominantly supported by recycled N, as evidenced by integrated euphotic zone f-ratios of <0.5 (Table 1). The one exception appears to be PS1 in September, where the $^{15}NO_3^-$ and $^{15}NH_4^+$–based f-ratio was 0.62; however, as detailed below, the "true" f-ratio at this station was likely <0.5, indicating a recycled N-supported system. Given the low to undetectable euphotic zone NO_3^- concentrations in September, a low f-ratio at both stations is to be expected, and is consistent with the observation that the September phytoplankton community was dominated by pico- and nanophytoplankton (<20 μm), including *Synechococcus* (Van Oostende et al. 2017), which tend to thrive under conditions of intense recycling (Dortch 1990; Chisholm 1992). The low f-ratios reconstructed for the May stations are arguably more surprising, as euphotic zone NO_3^- concentrations were non-limiting. However, NH_4^+ concentrations were fairly high,

and light may have been limiting, potentially explaining the apparent preference for NH_4^+ over NO_3^- at this time. The high ambient DIN levels and potential for light limitation suggest conditions generally found prior to the North Atlantic spring bloom. In any case, in both the late summer and the spring, our data suggest a subarctic North Atlantic ecosystem dominated by regenerated production.

Primary production in the subarctic North Atlantic

The absence of a clear relationship between NPP and NO_3^- uptake is perhaps not surprising given that C fixation and N uptake have been shown to be temporally decoupled in this region (Bury et al., 2001). The highest ^{13}C-based rate of euphotic zone integrated NPP was measured in late summer (September PS1), yet was more similar to (albeit on the low end of) rates measured at the North Atlantic Bloom Experiment (NABE) site (47°N, 20°W) during the spring (range of 79–164 mmol C m^{-2} d^{-1}; Bender et al., 1992; Buesseler et al., 1992; Joint et al., 1993; Martin et al., 1993; Bury et al., 2001) than the summer (range of 36–54 mmol C m^{-2} d^{-1}; Frazel and Berberian, 1990; Joint et al., 1993). By contrast, our springtime rates of NPP are low compared to previous measurements at the NABE site, and more similar to previously determined summer values.

Even though the rates of NPP varied with season, the POC concentrations were very similar at all stations (Figures 3 and 4), and when integrated over the euphotic zone, were slightly higher in May than September (Table 1). This suggests that the specific rates of carbon fixation (which approximate community growth rates) were lower in spring than in summer. Indeed, dividing the euphotic zone integrated rates of NPP by the POC concentrations yields specific carbon fixation rates of 0.11-0.16 d^{-1} in September and 0.06-0.08 d^{-1} in May. It is possible that the May biomass pool included a significant component of inactive detrital material, which would contribute to high POC concentrations but not to NPP, and would mean that we had underestimated the growth rates. However, detritus is usually carbon-rich, yet the measured biomass C:N ratios were similar to those expected for typical marine biomass (i.e., the "Redfield ratio") at all stations in both months (Table 2), strongly suggesting that a carbon-rich detrital pool cannot explain the seasonal differences in specific carbon fixation rates. Moreover, the community growth rates suggested by total N uptake rates normalized to PON concentrations in May (0.05-0.08 d^{-1}) are very similar to those calculated from the carbon data, verifying the carbon-based rates. We conclude that the community growth rates really were lower in May than in September, likely because the

water column had only recently become sufficiently stratified for phytoplankton growth to commence, the surface water temperature was ~4°C colder, and surface light levels were ~40% lower.

Nitrification in the upper subarctic North Atlantic

Measurements of NH_4^+ and NO_2^- oxidation are scarce in high latitude regions of the world ocean and have not previously been reported for the subarctic North Atlantic. The subsurface maxima in NH_4^+ and NO_2^- oxidation rates fell into the typical range of open ocean measurements (e.g., Ward and Zafiriou 1988; Raimbault et al. 1999; Sutka et al. 2004; Newell et al. 2013; Peng et al. 2016) and were observed just below the depth of 1% PAR at all stations during both seasons. Overall, NH_4^+ and NO_2^- oxidation rates in the euphotic zone were one to two orders of magnitude lower than the NO_3^- uptake rates (Figures 3 and 4; Table 1), suggesting that nitrification within the euphotic zone did not contribute significantly to the NO_3^- consumed by phytoplankton.

Low euphotic zone rates of NH_4^+ and NO_2^- oxidation have traditionally been attributed to photoinhibition (Horrigan et al. 1981; Olson 1981). The physiological basis for light sensitivity of ammonia-oxidizing bacteria (AOB) was assumed to be cytochrome damage (Ward 2011). However, cytochrome is not part of the electron transport system of ammonia-oxidizing archaea (AOA) (Walker et al. 2010; Santoro et al. 2015), which are now considered primarily responsible for NH_4^+ oxidation in marine environments (Beman et al. 2008; Santoro et al. 2010; Horak et al. 2013; Martens-Habbena et al. 2015; Peng et al. 2015). Two recent studies have demonstrated that AOA are inhibited by low levels of light (Merbt et al. 2012; Qin et al. 2014) and field-based studies have shown that reactive oxygen species commonly generated in the euphotic zone can inhibit the metabolic activity of AOA (Tolar et al. 2016; Kim et al. 2016; Horak et al. 2017). The mechanism inhibiting NH_4^+ oxidation by AOA, however, remains unresolved.

In addition to inhibition based on abiotic factors, substrate competition with phytoplankton has been suggested as an explanation for low or zero nitrification rates in the euphotic zone (Ward 1985, 2005; Smith et al. 2014). In both September and May, the rates of NH_4^+ oxidation were always lower than NH_4^+ uptake in the euphotic zone (Figure 3 and 4; Table 1). However, at the only depth below the euphotic zone where both NH_4^+ oxidation and uptake were measured (82 m at PS2 in May), the rate of NH_4^+ oxidation was twice that of uptake.

This is consistent with the hypothesis that phytoplankton exert a strong control on NH_4^+ oxidation by competing for substrate with NH_4^+ oxidizers in the euphotic zone but not below it where photosynthetic activity is low.

Although nitrification activity was generally low in the subarctic North Atlantic euphotic zone, there is evidence that regenerated NO_3^- could fuel a substantial portion of total primary production in oligotrophic ocean regions such as the subtropical gyres (Raimbault and Garcia 2008; Shiozaki et al. 2016). For example, in the North Pacific subtropical gyre, nitrification has been shown to contribute more than half of the NO_3^- assimilated on average (Shiozaki et al. 2016). Primary productivity in subtropical gyres is usually limited by fixed N, in particular due to the low supply of subsurface NO_3^- resulting from weak mixing and strong seasonal stratification. As a result, regenerated NO_3^- from nitrification within the mixed layer may play a relatively important role in total NO_3^- supply. Conversely, in highly productive regions of the ocean, strong vertical mixing in the water column replenishes the euphotic zone NO_3^-, dwarfing the contribution of regenerated NO_3^- from nitrification. Therefore, the contribution of nitrification to the euphotic zone NO_3^- supply may be expected to inversely correlate with primary productivity. Indeed, a compilation of field measurements confirms this trend (Figure 7), showing that when primary productivity is greater than 100 mmol C m^{-2} d^{-1}, nitrification generally contributes less than a quarter of the NO_3^- taken up by phytoplankton. On the other hand, when primary productivity is less than 100 mmol C m^{-2} d^{-1}, the contribution of nitrification to NO_3^- uptake is often greater than 10% but highly variable, suggesting that it also depends on other factors such as sampling season and location. A transect study from the North to South Atlantic also indicated a greater relative contribution of nitrification to NO_3^- supply under conditions of lower primary productivity in the gyres (Clark et al. 2008). However, recent work from the oligotrophic North Atlantic showed that NO_3^- uptake is always the dominant N cycle process in the euphotic zone, regardless of season, with nitrification becoming important only in the dark waters below it (Fawcett et al. 2015). The authors attribute this finding to the high affinity of N-limited phytoplankton for NH_4^+. Taken together, the above studies suggest that euphotic zone nitrification can only become proportionally significant as a NO_3^- source to phytoplankton when hydrographically-supplied NO_3^- has been essentially completely exhausted.

The variability of the MLD could constitute a physical process affecting the contribution of nitrification to NO_3^- uptake. At station PS1 in September and station PS2 in May, the mixed

layer occasionally penetrated below the depth of the euphotic zone (Figure 2) where NH_4^+ and NO_2^- oxidation rates were high (Figure 2). Such a fluctuation in MLD may transport recently regenerated NO_3^- into the euphotic zone, further complicating the accounting of new production on timescales of days to weeks. However, at least during our sampling period, these events of mixed layer deepening were short-lived. Given the relatively low rates of NH_4^+ and NO_2^- oxidation measured near the base of the euphotic zone, this would allow for only a small quantity of regenerated NO_3^- supply relative to the new NO_3^- entrained from below the mixed layer and the existing concentration within the mixed layer. Following the approach of Fawcett et al. (2015) for the Sargasso Sea, we turn to the dual isotopes of NO_3^- to gain insight into the longer-term importance of nitrification relative to subsurface NO_3^- supply to the euphotic zone.

The observed distribution of the N and O isotopes of NO_3^- is consistent with the vertical separation of NO_3^- uptake (in the euphotic zone) and nitrification (in the twilight zone waters below the euphotic zone) over the upper 500 m of the water column. Above 150-200 m, NO_3^- $\delta^{15}N$ and $\delta^{18}O$ rise in unison (along a 1:1 line) from the average $\delta^{15}N$ and $\delta^{18}O$ of the subsurface NO_3^- source (Figure 8). This trend is indicative of NO_3^- uptake by phytoplankton, which has been shown in culture to fractionate the N and O isotopes of NO_3^- in a ratio of 0.96-1.09 (Granger et al. 2004, 2010; Karsh et al. 2012). Below 150-250 m, there is a clear upward rise in the $\delta^{18}O$ of NO_3^- (by as much as 2.2‰) that is not accompanied by an increase in NO_3^- $\delta^{15}N$. This pattern is indicative of the co-occurrence of partial NO_3^- uptake and nitrification in the waters below the euphotic zone (Wankel et al. 2007; Sigman et al. 2009; Fawcett et al. 2015). As outlined in the introduction, the cycling of N between NO_3^- uptake and nitrification has little net effect on the $\delta^{15}N$ of NO_3^-. However, because the $\delta^{18}O$ of NO_3^- being consumed is initially lower than that produced by nitrification (-3.5‰ to -1.7‰, assuming an isotope effect estimated from the NO_3^- isotope data of 3.5‰ to 5.3‰), versus 1‰ to 2‰, the internal cycle of NO_3^- uptake and nitrification will cause NO_3^- $\delta^{18}O$ to drift upwards (Sigman et al. 2009; Buchwald and Casciotti 2013). The $\delta^{15}N$ and $\delta^{18}O$ of NO_3^- in the subarctic North Atlantic thus indicate that NO_3^- uptake is the dominant biological N transformation process in the euphotic zone, with nitrification becoming significant only in the dark waters below the euphotic zone. Our NO_3^- dual isotope data provide an integrated view of the late summer and spring N cycle in the North Atlantic that complements the *in situ* rate measurements. These data suggest that the results of the incubation experiments apply

beyond the short time period sampled here and confirm that in the spring through late summer, upper ocean nitrification in the subarctic North Atlantic is far slower than the upward rate of subsurface NO_3^- supply.

Even though euphotic zone nitrification was slow during our sampling period, it was detectable at times, and we can use the euphotic zone integrated measurements of NH_4^+ and NO_2^- oxidation to correct the ^{15}N-based rates of new production for regenerated NO_3^- uptake. NO_2^- oxidation is the step in the nitrification pathway that produces NO_3^-; this process accounts for a maximum of 5.1% of the assimilated euphotic zone NO_3^- at our stations (Table 1). Re-allocating 5.1% of new production to regenerated production decreases the average euphotic zone f-ratios by 0.01 to 0.03 (Eqn. 1) (i.e., a decrease in the fraction of export production of 1% to 3%). Repeating the same exercise for NH_4^+ oxidation yields an f-ratio decrease of 0.02 to 0.07. NH_4^+ oxidation is equivalent to a maximum of 10.9% of the NO_3^- uptake rate, although this increases to 16.4% if the integration depth at PS2 in May is extended to 82 m, and yields an f-ratio decrease of 0.03 to 0.10. This last calculation places an upper limit on the fraction of regenerated NO_3^- that could have been supplied to the euphotic zone at the time of our sampling because (1) the mixed layer never penetrated as deep as 82 m, and (2) NO_2^- rather than NH_4^+ oxidation is the N cycle process that actually produces regenerated NO_3^-. Regardless, despite arguments that NO_3^- uptake in oceanic surface waters is significantly higher than the flux of organic N out of the euphotic zone (Yool et al. 2007), both our *in situ* rate measurements and NO_3^- isotope data indicate that this is not the case in the late summer or springtime subarctic North Atlantic.

The vertical distribution of ammonium and nitrite oxidation

The observed pattern of subsurface maxima in NH_4^+ and NO_2^- oxidation rates is consistent with field measurements from other parts of the open ocean, including the eastern equatorial Pacific, the North Pacific, and the subtropical North Atlantic (e.g. Ward and Zafiriou 1988; Dore and Karl 1996; Beman et al. 2013; Newell et al. 2013). A common finding of all these studies is that the measured NO_2^- oxidation rates are typically lower than the coincident NH_4^+ oxidation rates, suggesting that the second step in the nitrification pathway is rate-limiting. This is contrary to the classical perception, based on the observation that NO_2^- does not usually accumulate in oxygenated waters, that NH_4^+ oxidation is rate-limiting (Kendall 1998). In the subarctic North Atlantic, euphotic zone integrated NH_4^+ oxidation rates were at 2.1 to 5.5 times the NO_2^- oxidation rates and a NO_2^- concentration maximum (as high as 0.6 μmol l$^-$

$^{-1}$) was evident at all stations (except PS1 in May, where NO_2^- concentrations were relatively high throughout the upper 200 m) (Figure 6A).

Differential light sensitivity of NH_4^+ and NO_2^- oxidizers is one possible reason for the higher rates of NH_4^+ versus NO_2^- oxidation. An early study showed that an isolated strain of NO_2^--oxidizing bacteria (NOB), *Nitrobacter winogradskyi*, was more light-sensitive than the AOB, *Nitrosomonas europaea* (Bock 1965). In seawater collected from the coastal waters of San Diego, CA, NO_2^- oxidation was completely inhibited even at low light levels (16.7 μE m^{-2} s^{-1}; equivalent to ~1% of typical surface PAR), whereas at the same light level, NH_4^+ oxidation declined to 70% of the dark rate (Olson 1981). There are no studies directly comparing the light sensitivity of marine AOA and NOB, but a recent physiological study of three marine AOA strains demonstrated that the degree of photoinhibition at 15 μE m^{-2} s^{-1} was less than 20% (Qin et al. 2014). Since AOA are probably responsible for most NH_4^+ oxidation in seawater (Beman et al. 2008; Santoro et al. 2010; Horak et al. 2013; Martens-Habbena et al. 2015; Peng et al. 2015), their lower sensitivity to light compared to NOB is likely a major reason for the observed higher rates of NH_4^+ oxidation than NO_2^- oxidation.

The peak in NO_2^- concentration observed at the base of the euphotic zone is termed the primary NO_2^- maximum (PNM) (Figure 6A), a feature that is ubiquitous in stratified aerobic water columns. While the depth of the PNM often overlaps with the NH_4^+ and NO_2^- oxidation maxima, an imbalance in the rates of these two processes is not the only possible mechanism that could sustain it (Lomas and Lipschultz 2006, and references therein). It has been hypothesized that phytoplankton (and even some bacteria) may release NO_2^- deriving from the incomplete assimilatory reduction of NO_3^- under conditions of light limitation (Kiefer et al. 1976; Wada and Hattori 1978; Collos 1998). This hypothesis garners support from the vertical distribution of NO_2^- in the water column, since the highest concentrations tend to occur at depths with light levels ≤1% PAR. Of course, NH_4^+ oxidation occurring at a rate unmatched by NO_2^- oxidation, perhaps due to differential light inhibition of AOA/AOB versus NOB (Olson 1981), is also consistent with the vertical distribution of NO_2^-.

The $\delta^{15}N$ of NO_2^- may help to elucidate the origin of the PNM. In September, NO_2^- $\delta^{15}N$ calculated via mass balance ranged from -8.0 ± 3.3‰ to -2.7 ± 1.1‰, while in May, NO_2^- $\delta^{15}N$ was significantly lower at -31.6 ± 12.0‰ to -19.7 ± 8.6‰ (Figure 6B). Assuming an

isotope effect of 5.2‰, as implied by the NO_3^- isotope data, NO_2^- efflux by phytoplankton taking up NO_3^- with an initial $\delta^{15}N$ of 4.8‰ (Figure 5A, C) would yield NO_2^- with a mean $\delta^{15}N$ of -1.6‰ in both September and May (Supplementary Information). By contrast, the combined isotope effects of NH_4^+ and NO_2^- oxidation would generate NO_2^- with a $\delta^{15}N$ of -30.5‰ to 2.7‰ in September and -34.0‰ to -2.0‰ in May (Casciotti 2009). While the results of this exercise are less conclusive for September than for May, they nonetheless suggest that the PNM derives mainly from NH_4^+ oxidation since this process can drive NO_2^- $\delta^{15}N$ to the very low values estimated for subarctic North Atlantic waters (Figure 6B).

Implications of other N cycle processes for estimates of new and regenerated production

In addition to nitrification, there are other N cycle processes that may complicate equating NO_3^- and NH_4^+ uptake with new and regenerated production (Dugdale and Goering 1967; Bronk et al. 1994). For example, new N is also supplied to oceanic surface waters through N_2 fixation and atmospheric N deposition (Owens et al. 1992; Capone et al. 2005), and dissolved organic N (DON) can be a significant source of regenerated N to phytoplankton (see review by Bronk 2002). In theory, if NPP measured using ^{13}C tracer experiments is supported mainly by NO_3^- and NH_4^+, then the total rate of N uptake (i.e., $\rho_{NO3}+\rho_{NH4}$) multiplied by an appropriate biomass C:N ratio should approximate the ^{13}C-based rate of NPP.

Multiplying the euphotic zone integrated rates of total N uptake at each station by the corresponding average biomass C:N ratio (Table 2) reveals that NPP in May is well represented by the sum of NO_3^-- and NH_4^+-based production, while in September, ~50% of the total carbon production is unaccounted for by NO_3^- and NH_4^+ uptake (Figure 9). One consideration is that previous work at the NABE site (47°N; 20°W) has shown a decoupling of NPP and N uptake, with the maximum rate of N uptake preceding that of carbon fixation by three days (Bury et al. 2001). We cannot rule out the possibility that such a decoupling is at least partly responsible for the discrepancies we observe, although the Redfield-like composition of the biomass suggests that the growth of the phytoplankton community was roughly balanced at the time of our experiments. The calculation above implies that the f-ratios calculated for May provide a reasonable estimate of the potentially exportable fraction of NPP (which, by multiplying ρ_{NO3_integ} by the measured biomass C:N ratio at each station amounts to an export flux of roughly 22 mmol C m^{-2} d^{-1} at PS1 and 37 mmol C m^{-2} d^{-1} at PS2). By contrast, we have no way of evaluating the accuracy of the f-ratios calculated for

September. If all of the summertime NPP that is unaccounted for by our measurements of NO_3^- and NH_4^+ uptake were supported by a new N source, the f-ratio would increase to 0.83 at PS1 and 0.71 at PS2. If, on the other hand, the "missing" N source were entirely regenerated, the f-ratio would decline to 0.29 at PS1 and 0.10 at PS2.

The Atlantic Ocean is thought to be responsible for 10-25% (Großkopf et al. 2012; Luo et al. 2012; Benavides and Voss 2015) of the 100-200 Tg N supplied to the ocean annually by marine N_2 fixation (Deutsch et al. 2007; Gruber and Galloway 2008). Modeling and geochemical studies suggest that almost all of this N_2 fixation occurs in the equatorial and subtropical North Atlantic, with very little N_2 fixation north of 40°N (Coles and Hood 2006; Deutsch et al. 2007; Marconi et al. 2017). The only incubation-based measurements of N_2 fixation conducted near our study region, albeit significantly further south (42.55°N; 19.84°W), suggest a maximum euphotic zone integrated N_2 fixation rate of 3.4-8.0 μmol N m^{-2} d^{-1} (Rees et al. unpublished, included in Luo et al., 2012). Assuming parallel cycling of N and C, this could support the fixation of 21-50 μmol C m^{-2} d^{-1}, which is <0.25% of the NPP that is apparently unsupported by NO_3^- and NH_4^+ uptake (~23-41 mmol C m^{-2} d^{-1}). It is thus very unlikely that N_2 fixation fueled a significant fraction of the "excess" NPP measured in September.

Atmospheric N deposition is another potential new N source to surface waters (Duce et al. 2008). The upper bound on total atmospheric N deposition (i.e., the sum of wet and dry organic and inorganic N) in the vicinity of our stations has been estimated at 47 μmol N m^{-2} d^{-1} (Spokes et al. 2000; Baker et al. 2006, 2010). This amounts to a carbon fixation rate of ~300 μmol C m^{-2} d^{-1}, which, like N_2 fixation, is insignificant (<1.5%) relative to the quantity of NPP unaccounted for by our N budget. We thus do not appear to be missing a source of new N to the late summer subarctic North Atlantic, and instead turn to the possible regenerated N forms.

NH_4^+ regeneration during the uptake experiments can potentially result in the production of unlabeled NH_4^+ in the incubation bottles, effectively diluting the $^{15}N/^{14}N$ of the NH_4^+ pool being assimilated and leading to an underestimate of the NH_4^+ uptake rates (Glibert et al. 1982, 1992; Kanda et al. 1987; Lipschultz 2008). While our short incubation period was designed to minimize this effect (Glibert et al. 1982; Kanda et al. 1987), we cannot rule out the possibility that the $^{15}NH_4^+$ uptake rates measured in September underestimate the true

NH_4^+ uptake rates, potentially accounting for some fraction of the "missing" N supporting NPP at this time. However, in order to fully account for the excess NPP, NH_4^+ uptake would need to be underestimated by 110-300%.

Dissolved organic N (DON) can constitute the largest fixed N pool in oceanic surface waters, although much of it remains uncharacterized (Bronk 2002). While historically considered mostly recalcitrant, work over the last two decades has shown that the fluxes into and out of the DON pool are significant, and that phytoplankton may fuel a substantial portion of their growth through various forms of DON (Bronk et al. 2007). These include highly labile compounds such as urea and dissolved free amino acids (DFAAs), which have a turnover time of minutes to days (Fuhrman 1987; Jørgensen et al. 1993; Bronk et al. 1998), and less labile compounds such as proteins and amino polysaccharides that turn over on a timescale of months to years (Bronk 2002; Bronk et al. 2007). Because of the chemical complexity of the DON pool, direct measurements of its consumption are difficult. Nonetheless, coastal phytoplankton have been shown to rely on urea and DFAAs for up to 80% of their N (Harrison et al. 1985; Glibert et al. 1991; Berg et al. 2001) and DON has been estimated to support 30-50% of the daily N requirements of phytoplankton in the equatorial Pacific (Benner et al. 1997). Uptake rates of urea of 45 nmol l^{-1} d^{-1} (specific uptake (V_{urea}) of 0.05 d^{-1}) have been measured in the North Atlantic (Varela et al. 2005), while rates as high as 88 nmol l^{-1} d^{-1} and 165 nmol l^{-1} d^{-1} (V_{urea} of 0.12 d^{-1} to 0.14 d^{-1}) have been measured in the North Sea (Riegman and Noordeloos 1998) and subarctic Pacific (Wheeler and Kokkinakis 1990), respectively. If urea were consumed at these specific rates in the subarctic North Atlantic in September, it could account for 48-194% of the "missing" N at PS1 and 52-210% at PS2 (i.e., V_{urea} (d^{-1}) x $[PON]_{integrated}$ (mmol m^{-2}) x C:N = mmol C m^{-2} d^{-1}).

Given that urea is just one component of the DON pool, the simple calculation above illustrates that DON could easily fuel 50% of NPP in September. Moreover, there is some evidence that phytoplankton rely more heavily on DON during the summer and fall when ambient NO_3^- concentrations reach a minimum (Paerl 1991; Berg et al. 2003). This is consistent with our observations of very low euphotic zone NO_3^- in September, particularly at PS2. In addition, most of the chlorophyll at the late summer stations was measured in the <2 μm (60-75%) and 2-20 μm (20-35%) phytoplankton size fractions, indicating a community dominated by cyanobacteria and pico- and nanoeukaryotes (Van Oostende et al. 2017). These phytoplankton groups tend to dominate the autotrophic assemblage later in the growing

season (Lochte et al. 1993; Dandonneau et al. 2004; Barton et al. 2013) and are often associated with increased DON (e.g., urea) uptake (Berg et al. 1997). This is in contrast to larger diatoms that bloom earlier in the season in response to high NO_3^- and silicate inputs (Lochte et al. 1993; Alkire et al. 2014; Cetinić et al. 2015).

The concentration and $\delta^{15}N$ of DON show remarkable stability in the subtropical North Atlantic (Hansell and Carlson 2001; Knapp et al. 2005, 2011) and elsewhere (e.g., Letscher et al. 2013), which might be taken as contrary to the evidence for significant DON uptake presented here. One potential explanation is that the DON compounds that are rapidly assimilated in the North Atlantic euphotic zone are also being produced rapidly in the same waters. If so, these rapidly recycled compounds would be important for phytoplankton nutrition without ever representing a substantial portion of the standing DON pool. In this scenario, the bulk of the measurable DON pool is not involved in the rapid cycling, perhaps because it is biochemically refractory.

A potential complication to the argument for DON uptake supporting 50% of late summer production is that phytoplankton have been observed to release upwards of 25% of the NO_3^- and NH_4^+ they assimilate as DON (Bronk et al. 1994; Bronk 1999; Bronk and Ward 2000). In ^{15}N tracer experiments, this means that ^{15}N-labeled DON deriving from $^{15}NH_4^+$ or $^{15}NO_3^-$ uptake that is released into the extracellular DON pool will be excluded from ^{15}N-based rate calculations (Bronk et al. 1994), assuming that none of the $DO^{15}N$ is re-assimilated by the incubating phytoplankton. To address this, we calculated the total concentration of ^{15}N at the beginning and end of each $^{15}NO_3^-$ or $^{15}NH_4^+$ experiment (after Bronk and Glibert 1994). We recovered an average of 99 ± 12% of the ^{15}N that was added, which suggests that N loss to the DON pool during our experiments was minimal.

In sum, the most likely explanation for measured rates of NPP in late summer that far exceed those implied by concurrent NO_3^- and NH_4^+ uptake experiments is that a phytoplankton community dominated by small cells grew partly on a regenerated N form (e.g., urea and/or other forms of DON) that we did not track. One implication is that regenerated production at PS1 and PS2 in late summer was significantly higher than that suggested by measurements of $^{15}NH_4^+$ uptake, and that the f-ratios at these stations are more likely to be on the order of

0.10-0.29 (see above) than the higher values that we initially calculated on the basis of $^{15}NO_3^-$ and $^{15}NH_4^+$ uptake alone (Table 1).

Conclusions

In the subarctic North Atlantic Ocean, we measured low but detectable rates of NH_4^+ and NO_2^- oxidation in the euphotic zone in late summer and late spring. Nevertheless, nitrification integrated over the euphotic zone accounted for only a small fraction (less than a maximum of 11%) of the NO_3^- taken up by phytoplankton, as indicated by both short-term rate measurements and the natural abundance N and O isotopes of NO_3^-, which integrate over a longer time-period. We conclude that in the subarctic North Atlantic the strength of the biological pump approximated by the ratio of NO_3^- uptake relative to NO_3^-+NH_4^+ uptake (i.e., the f-ratio) does not significantly overestimate N export compared to the case where euphotic zone nitrification is neglected. This finding is consistent with previous measurements in productive subpolar regions of the ocean and is likely due to the high rate of subsurface NO_3^- supply, high growth rates of phytoplankton under N-replete conditions, and superior affinity of phytoplankton for NH_4^+ compared to nitrifying bacteria/archaea under irradiances typical of the euphotic zone. However, other sources of regenerated N not measured in this study, such as various forms of DON, may have supported as much as half of the primary production measured in the region in late summer. Therefore, the f-ratio approximated by $^{15}NH_4^+$ and $^{15}NO_3^-$ uptake should still be interpreted with caution despite the negligible contribution of nitrification to the euphotic zone NO_3^- pool. In addition, the vertical distribution of and the consistently higher NH_4^+ oxidation rates compared to NO_2^- oxidation rates in our study suggest that NO_2^- oxidation may be the rate-limiting step of nitrification in the upper water column of the open ocean. Along with the N isotopes of NO_2^-, this uncoupling between NH_4^+ and NO_2^- oxidation indicates that nitrification probably contributes to the formation of the primary NO_2^- maximum in the subarctic North Atlantic, at least in spring and summer.

Acknowledgements

We are grateful to Q. Ji, Andrew R. Babbin, Aimee R. Babbin, M. Woodward, A. Sabadel, J. Lueders-Dumont, J. Hoffman for their shipboard assistance in nutrient concentration measurements, sample collection, and incubation experiments, and to the captain and crew of the R/V Endeavor for a successful cruise. We thank M. Weigand and S. Oleynik for their assistance with the denitrifier-related work and mass spectrometry measurements, K.

Casciotti for providing the NO_2^- stable isotope standard, and Bror Jonnson for the satellite data. This work was supported by NSF fund National Science Foundation Grant no. OCE-1136345 to B.B. Ward and D.M. Sigman.

References

Alkire, M. B., C. Lee, E. D'Asaro, M. J. Perry, N. Briggs, I. Cetinić, and A. Gray. 2014. Net community production and export from Seaglider measurements in the North Atlantic after the spring bloom. J. Geophys. Res. Oceans **119**: 6121–6139. doi:10.1002/2014JC010105

Altabet, M. A., and L. F. Small. 1990. Nitrogen isotopic ratios in fecal pellets produced by marine Zooplankton. Geochim. Cosmochim. Acta **54**: 155–163. doi:10.1016/0016-7037(90)90203-W

Bagniewski, W., K. Fennel, M. J. Perry, and E. A. D'Asaro. 2011. Optimizing models of the North Atlantic spring bloom using physical, chemical and bio-optical observations from a Lagrangian float. Biogeosciences **8**: 1291–1307. doi:10.5194/bg-8-1291-2011

Baker, A. R., T. D. Jickells, K. F. Biswas, K. Weston, and M. French. 2006. Nutrients in atmospheric aerosol particles along the Atlantic Meridional Transect. Deep Sea Res. Part II Top. Stud. Oceanogr. **53**: 1706–1719. doi:10.1016/j.dsr2.2006.05.012

Baker, A. R., T. Lesworth, C. Adams, T. D. Jickells, and L. Ganzeveld. 2010. Estimation of atmospheric nutrient inputs to the Atlantic Ocean from 50°N to 50°S based on large-scale field sampling: Fixed nitrogen and dry deposition of phosphorus. Glob. Biogeochem. Cycles **24**: GB3006. doi:10.1029/2009GB003634

Barton, A. D., Z. V. Finkel, B. A. Ward, D. G. Johns, and M. J. Follows. 2013. On the roles of cell size and trophic strategy in North Atlantic diatom and dinoflagellate communities. Limnol. Oceanogr. **58**: 254–266. doi:10.4319/lo.2013.58.1.0254

Beman, J. M., B. N. Popp, and C. A. Francis. 2008. Molecular and biogeochemical evidence for ammonia oxidation by marine Crenarchaeota in the Gulf of California. ISME J. **2**: 429–441. doi:10.1038/ismej.2007.118

Beman, J. M., B. N. Popp, and S. E. Alford. 2012. Quantification of ammonia oxidation rates and ammonia-oxidizing archaea and bacteria at high resolution in the Gulf of California and eastern tropical North Pacific Ocean. Limnol. Oceanogr. **57**: 711–726. doi:10.4319/lo.2012.57.3.0711

Beman, J. M., J. Leilei Shih, and B. N. Popp. 2013. Nitrite oxidation in the upper water column and oxygen minimum zone of the eastern tropical North Pacific Ocean. ISME J. **7**: 2192–2205. doi:10.1038/ismej.2013.96

Benavides, M., and M. Voss. 2015. Five decades of N2 fixation research in the North Atlantic Ocean. Front. Mar. Sci. **2**. doi:10.3389/fmars.2015.00040

Benner, R., B. Biddanda, B. Black, and M. McCarthy. 1997. Abundance, size distribution, and stable carbon and nitrogen isotopic compositions of marine organic matter isolated by tangential-flow ultrafiltration. Mar. Chem. **57**: 243–263. doi:10.1016/S0304-4203(97)00013-3

Berg, G. M., M. Balode, I. Purina, S. Bekere, C. Bchemin, and S. Y. Maestrini. 2003. Plankton community composition in relation to availability and uptake of oxidized and reduced nitrogen. Aquat. Microb. Ecol. **30**: 263–274. doi:10.3354/ame030263

Berg, G. M., P. M. Glibert, N. O. G. Jørgensen, M. Balode, and I. Purina. 2001. Variability in inorganic and organic nitrogen uptake associated with riverine nutrient input in the Gulf of Riga, Baltic Sea. Estuaries **24**: 204–214. doi:10.2307/1352945

Berg, G. M., P. M. Glibert, M. W. Lomas, and M. A. Burford. 1997. Organic nitrogen uptake and growth by the chrysophyte Aureococcus anophagefferens during a brown tide event. Mar. Biol. **129**: 377–387. doi:10.1007/s002270050178

Bock, E. 1965. Vergleichende Untersuchungen über die Wirkung sichtbaren Lichtes auf Nitrosomonas europaea und Nitrobacter winogradskyi. Arch. Für Mikrobiol. **51**: 18–41. doi:10.1007/BF00406848

Boyd, P., A. Pomroy, S. Bury, G. Savidge, and I. Joint. 1997. Micro-algal carbon and nitrogen uptake in post-coccolithophore bloom conditions in the northeast Atlantic, July 1991. Deep Sea Res. Part Oceanogr. Res. Pap. **44**: 1497–1517. doi:10.1016/S0967-0637(97)00039-3

de Boyer Montégut, C., G. Madec, A. S. Fischer, A. Lazar, and D. Iudicone. 2004. Mixed layer depth over the global ocean: An examination of profile data and a profile-based climatology. J. Geophys. Res. Oceans **109**: C12003. doi:10.1029/2004JC002378

Braman, R. S., and S. A. Hendrix. 1989. Nanogram nitrite and nitrate determination in environmental and biological materials by vanadium(III) reduction with chemiluminescence detection. Anal. Chem. **61**: 2715–2718. doi:10.1021/ac00199a007

Bronk, D. A. 1999. Rates of NH 4+ uptake, intracellular transformation and dissolved organic nitrogen release in two clones of marine Synechococcus spp. J. Plankton Res. **21**: 1337–1353.

Bronk, D. A. 2002. Dynamics of DON. Biogeochem. Mar. Dissolved Org. Matter **384**: p153–247.

Bronk, D. A., and P. M. Glibert. 1994. The fate of the missing 15N differs among marine systems. Limnol. Oceanogr. **39**: 189–195. doi:10.4319/lo.1994.39.1.0189

Bronk, D. A., P. M. Glibert, T. C. Malone, S. Banahan, and E. Sahlsten. 1998. Inorganic and organic nitrogen cycling in Chesapeake Bay: autotrophic versus heterotrophic processes and relationships to carbon flux. Aquat. Microb. Ecol. **15**: 177–189. doi:10.3354/ame015177

Bronk, D. A., P. M. Glibert, B. B. Ward, and others. 1994. Nitrogen uptake, dissolved organic nitrogen release, and new production. Sci.-N. Y. THEN Wash.- 1843–1843.

Bronk, D. A., J. H. See, P. Bradley, and L. Killberg. 2007. DON as a source of bioavailable nitrogen for phytoplankton. Biogeosciences **4**: 283–296.

Bronk, D. A., and D. K. Steinberg. "Nitrogen regeneration." *Nitrogen in the Marine Environment* (2008). doi:10.1016/B978-0-12-372522-6.00008-6

Bronk, D. A., and B. B. Ward. 2000. Magnitude of dissolved organic nitrogen release relative to gross nitrogen uptake in marine systems. Limnol. Oceanogr. **45**: 1879–1883. doi:10.4319/lo.2000.45.8.1879

Buchwald, C., and K. L. Casciotti. 2013. Isotopic ratios of nitrite as tracers of the sources and age of oceanic nitrite. Nat. Geosci. **6**: 308–313. doi:10.1038/ngeo1745

Buchwald, C., A. E. Santoro, M. R. McIlvin, and K. L. Casciotti. 2012. Oxygen isotopic composition of nitrate and nitrite produced by nitrifying cocultures and natural marine assemblages. Limnol. Oceanogr. **57**: 1361–1375. doi:10.4319/lo.2012.57.5.1361

Buesseler, K. O., M. P. Bacon, J. Kirk Cochran, and H. D. Livingston. 1992. Carbon and nitrogen export during the JGOFS North Atlantic Bloom experiment estimated from 234Th: 238U disequilibria. Deep Sea Res. Part Oceanogr. Res. Pap. **39**: 1115–1137. doi:10.1016/0198-0149(92)90060-7

Bury, S. J., P. W. Boyd, T. Preston, G. Savidge, and N. J. P. Owens. 2001. Size-fractionated primary production and nitrogen uptake during a North Atlantic phytoplankton bloom: implications for carbon export estimates. Deep Sea Res. Part Oceanogr. Res. **48**: 689–720. doi:10.1016/S0967-0637(00)00066-2

Capone, D. G., J. A. Burns, J. P. Montoya, A. Subramaniam, C. Mahaffey, T. Gunderson, A. F. Michaels, and E. J. Carpenter. 2005. Nitrogen fixation by Trichodesmium spp.: An important source of new nitrogen to the tropical and subtropical North Atlantic Ocean. Glob. Biogeochem. Cycles **19**: GB2024. doi:10.1029/2004GB002331

Casciotti, K. L. 2009. Inverse kinetic isotope fractionation during bacterial nitrite oxidation. Geochim. Cosmochim. Acta 73: 2061–2076. doi:10.1016/j.gca.2008.12.022

Casciotti, K. L., and M. R. McIlvin. 2007. Isotopic analyses of nitrate and nitrite from reference mixtures and application to Eastern Tropical North Pacific waters. Mar. Chem. **107**: 184–201. doi:10.1016/j.marchem.2007.06.021

Casciotti, K. L., D. M. Sigman, M. G. Hastings, J. K. Böhlke, and A. Hilkert. 2002. Measurement of the Oxygen Isotopic Composition of Nitrate in Seawater and Freshwater Using the Denitrifier Method. Anal. Chem. **74**: 4905–4912. doi:10.1021/ac020113w

Cavagna, A. J., F. Fripiat, M. Elskens, and others. 2015. Production regime and associated N cycling in the vicinity of Kerguelen Island, Southern Ocean. Biogeosciences **12**: 6515–6528. doi:10.5194/bg-12-6515-2015

Cetinić, I., M. J. Perry, E. D'Asaro, N. Briggs, N. Poulton, M. E. Sieracki, and C. M. Lee. 2015. A simple optical index shows spatial and temporal heterogeneity in phytoplankton community composition during the 2008 North Atlantic Bloom Experiment. Biogeosciences **12**: 2179–2194. doi:10.5194/bg-12-2179-2015

Chisholm, S. W. 1992. Phytoplankton Size, p. 213–237. *In* P.G. Falkowski, A.D. Woodhead, and K. Vivirito [eds.], Primary Productivity and Biogeochemical Cycles in the Sea. Springer US.

Clark, D. R., A. P. Rees, and I. Joint. 2008. Ammonium regeneration and nitrification rates in the oligotrophic Atlantic Ocean: Implications for new production estimates. Limnol. Oceanogr. **53**: 52–62. doi:10.4319/lo.2008.53.1.0052

Clark, D. R., C. E. Widdicombe, A. P. Rees, and E. M. S. Woodward. 2016. The significance of nitrogen regeneration for new production within a filament of the Mauritanian upwelling system. Biogeosciences **13**: 2873–2888. doi:10.5194/bg-13-2873-2016

Coles, V. J., and R. R. Hood. 2006. Modeling the impact of iron and phosphorus limitations on nitrogen fixation in the Atlantic Ocean. Biogeosciences Discuss. **3**: 1391–1451.

Collos, Y. 1998. Nitrate uptake, nitrite release and uptake, and new production estimates. Mar. Ecol. Prog. Ser. **171**: 293–301. doi:10.3354/meps171293

Craig, H., and L. I. Gordon. 1965. Deuterium and oxygen-18 variations in the ocean and marine atmosphere, p. 9–130. *In* Stable Isotopes in Oceanographic Studies and Paleo-Temperatures. Laboratorio di Geologia Nucleare.

Cullen, J. J. 2001. Primary production methods. Mar. Ecol. Prog. Ser. **52**: 2277–2284.

Dandonneau, Y., P.-Y. Deschamps, J.-M. Nicolas, H. Loisel, J. Blanchot, Y. Montel, F. Thieuleux, and G. Bécu. 2004. Seasonal and interannual variability of ocean color and composition of phytoplankton communities in the North Atlantic, equatorial Pacific and South Pacific. Deep Sea Res. Part II Top. Stud. Oceanogr. **51**. doi:10.1016/j.dsr2.2003.07.018

Deutsch, C., J. L. Sarmiento, D. M. Sigman, N. Gruber, and J. P. Dunne. 2007. Spatial coupling of nitrogen inputs and losses in the ocean. Nature **445**: 163–167. doi:10.1038/nature05392

DiFiore, P. J., D. M. Sigman, and R. B. Dunbar. 2009. Upper ocean nitrogen fluxes in the Polar Antarctic Zone: Constraints from the nitrogen and oxygen isotopes of nitrate. Geochem. Geophys. Geosystems 10: Q11016. doi:10.1029/2009GC002468

Dore, J. E., and D. M. Karl. 1996. Nitrification in the euphotic zone as a source for nitrite, nitrate, and nitrous oxide at Station ALOHA. Limnol. Oceanogr. **41**: 1619–1628. doi:10.4319/lo.1996.41.8.1619

Dortch, Q. 1990. The interaction between ammonium and nitrate uptake in phytoplankton. Mar. Ecol. Prog. Ser. **61**: 183–201.

Duce, R. A., J. LaRoche, K. Altieri, and others. 2008. Impacts of Atmospheric Anthropogenic Nitrogen on the Open Ocean. Science **320**: 893–897. doi:10.1126/science.1150369

Dugdale, R. C., and J. J. Goering. 1967. Uptake of New and Regenerated Forms of Nitrogen in Primary Productivity1. Limnol. Oceanogr. **12**: 196–206. doi:10.4319/lo.1967.12.2.0196

Eppley, R. W., and B. J. Peterson. 1979. Particulate organic matter flux and planktonic new production in the deep ocean. Nature **282**: 677–680. doi:10.1038/282677a0

Fawcett, S. E., M. W. Lomas, J. R. Casey, B. B. Ward, and D. M. Sigman. 2011. Assimilation of upwelled nitrate by small eukaryotes in the Sargasso Sea. Nat. Geosci. **4**: 717–722. doi:10.1038/ngeo1265

Fawcett, S. E., B. B. Ward, M. W. Lomas, and D. M. Sigman. 2015. Vertical decoupling of nitrate assimilation and nitrification in the Sargasso Sea. Deep-Sea Res. Part I **Complete**: 64–72. doi:10.1016/j.dsr.2015.05.004

Fernández, I. C. 2003. Cycle de l'azote et production primaire dans l'Atlantique Nord—Est: suivi saisonnier et influence de la meso echelle. Doctoral dissertation. Universite de la Mediterranee - Aix Marseille II.

Frazel, D. W., and G. Berberian. 1990. Distributions of chlorophyll and primary productivity in relation to water column structure in the eastern North Atlantic Ocean. Glob. Biogeochem. Cycles **4**: 241–251. doi:10.1029/GB004i003p00241

Fuhrman, J. 1987. Close coupling between release and uptake of dissolved free amino acids in seawater studied by an isotope dilution approach. Mar Ecol Prog Ser **37**: 45–52.

Garcia, H. E., R. A. Locarnini, T. P. Boyer, J. I. Antonov, O. K. Baranova, M. M. Zweng, J. R. Reagan, and D. R. Johnson. World Ocean Atlas 2013, Volume 4: Dissolved Inorganic Nutrients (phosphate, nitrate, silicate), edited by: Levitus, S. NOAA Atlas NESDIS 25.

Garside, C. 1982. A chemiluminescent technique for the determination of nanomolar concentrations of nitrate and nitrite in seawater. Mar. Chem. **11**: 159–167. doi:10.1016/0304-4203(82)90039-1

Glibert, P. M., D. C. Biggs, and J. J. McCarthy. 1982. Utilization of ammonium and nitrate during austral summer in the Scotia Sea. Deep Sea Res. Part Oceanogr. Res. Pap. **29**: 837–850. doi:10.1016/0198-0149(82)90049-8

Glibert, P. M., C. Garside, J. A. Fuhrman, and M. R. Roman. 1991. Dependent coupling of inorganic and organic nitrogen uptake and regeneration in the plume of the Chesapeake Bay estuary and its regulation by large heterotrophs. Limnol. Oceanogr. **36**: 895–909. doi:10.4319/lo.1991.36.5.0895

Glibert, P. M., C. A. Miller, C. Garside, M. R. Roman, and G. B. McManus. 1992. NH 4 + regeneration and grazing: interdependent processes in size-fractionated 15 NH 4 + experiments. Mar. Ecol. Prog. Ser. **82**: 65–74.

Granger, J., and D. M. Sigman. 2009. Removal of nitrite with sulfamic acid for nitrate N and O isotope analysis with the denitrifier method. Rapid Commun. Mass Spectrom. **23**: 3753–3762. doi:10.1002/rcm.4307

Granger, J., D. M. Sigman, J. A. Needoba, and P. J. Harrison. 2004. Coupled nitrogen and oxygen isotope fractionation of nitrate during assimilation by cultures of marine phytoplankton. Limnol. Oceanogr. **49**: 1763–1773. doi:10.4319/lo.2004.49.5.1763

Granger, J., D. M. Sigman, M. M. Rohde, M. T. Maldonado, and P. D. Tortell. 2010. N and O isotope effects during nitrate assimilation by unicellular prokaryotic and eukaryotic plankton cultures. Geochim. Cosmochim. Acta **74**: 1030–1040.

Großkopf, T., W. Mohr, T. Baustian, and others. 2012. Doubling of marine dinitrogen-fixation rates based on direct measurements. Nature **488**: 361–364. doi:10.1038/nature11338

Gruber, N., and J. N. Galloway. 2008. An Earth-system perspective of the global nitrogen cycle. Nature **451**: 293–296. doi:10.1038/nature06592

Hansell, D. A., and C. A. Carlson. 2001. Biogeochemistry of total organic carbon and nitrogen in the Sargasso Sea: control by convective overturn. Deep Sea Res. Part II Top. Stud. Oceanogr. 48: 1649–1667. doi:10.1016/S0967-0645(00)00153-3

Harrison, W. G., E. J. H. Head, R. J. Conover, A. R. Longhurst, and D. D. Sameoto. 1985. The distribution and metabolism of urea in the eastern Canadian Arctic. Deep Sea Res. Part Oceanogr. Res. Pap. **32**: 23–42. doi:10.1016/0198-0149(85)90015-9

Holmes, R. M., A. Aminot, R. Kérouel, B. A. Hooker, and B. J. Peterson. 1999. A simple and precise method for measuring ammonium in marine and freshwater ecosystems. Can. J. Fish. Aquat. Sci. **56**: 1801–1808. doi:10.1139/f99-128

Honjo, S., and S. J. Manganini. 1993. Annual biogenic particle fluxes to the interior of the North Atlantic Ocean; studied at 34°N 21°W and 48°N 21°W. Deep Sea Res. Part II Top. Stud. Oceanogr. **40**: 587–607. doi:10.1016/0967-0645(93)90034-K

Hooper, A. B., and K. R. Terry. 1974. Photoinactivation of Ammonia Oxidation in Nitrosomonas. J. Bacteriol. **119**: 899–906.

Horak, R. E. A., W. Qin, A. J. Schauer, E. V. Armbrust, A. E. Ingalls, J. W. Moffett, D. A. Stahl, and A. H. Devol. 2013. Ammonia oxidation kinetics and temperature sensitivity of a natural marine community dominated by Archaea. ISME J. **7**: 2023–2033. doi:10.1038/ismej.2013.75

Horak, R. E. A., W. Qin, A. D. Bertagnolli, and others. 2017. Relative impacts of light, temperature, and reactive oxygen on thaumarchaeal ammonia oxidation in the North Pacific Ocean. Limnol. Oceanogr. doi:10.1002/lno.10665

Horrigan, S. G., A. F. Carlucci, and P. M. Williams. 1981. Light inhibition of nitrification in sea-surface films. J. Mar. Res.

Hydes, D., M. Aoyama, A. Aminot, and others. 2010. Determination of dissolved nutrients (N, P, Si) in seawater with high precision and inter-comparability using gas-segmented continuous flow analysers.

Joint, I., A. Pomroy, G. Savidge, and P. Boyd. 1993. Size-fractionated primary productivity in the northeast Atlantic in May–July 1989. Deep Sea Res. Part II Top. Stud. Oceanogr. **40**: 423–440. doi:10.1016/0967-0645(93)90025-I

Jones, R. D. 1991. An improved fluorescence method for the determination of nanomolar concentrations of ammonium in natural waters. Limnol. Oceanogr. **36**: 814–819. doi:10.4319/lo.1991.36.4.0814

Jørgensen, N. O. G., N. Kroer, R. B. Coffin, X.-H. Yang, and C. Lee. 1993. Dissolved free amino acids, combined amino acids, and DNA as sources of carbon and nitrogen to marine bacteria. Mar. Ecol. Prog. Ser. **98**: 135–148.

Kanda, J., E. A. Laws, T. Saino, and A. Hattori. 1987. An evaluation of isotope dilution effect from conventional data sets of 15 N uptake experiments. J. Plankton Res. **9**: 79–90. doi:10.1093/plankt/9.1.79

Karsh, K. L., J. Granger, K. Kritee, and D. M. Sigman. 2012. Eukaryotic Assimilatory Nitrate Reductase Fractionates N and O Isotopes with a Ratio near Unity. Environ. Sci. Technol. **46**: 5727–5735. doi:10.1021/es204593q

Kendall, C. 1998. Chapter 16 - Tracing Nitrogen Sources and Cycling in Catchments, p. 519–576. *In* Isotope Tracers in Catchment Hydrology. Elsevier.

Kiefer, D. A., R. J. Olson, and O. Holm-Hansen. 1976. Another look at the nitrite and chlorophyll maxima in the central North Pacific. Deep Sea Res. Oceanogr. Abstr. **23**: 1199–1208. doi:10.1016/0011-7471(76)90895-0

Kim, J.-G., S.-J. Park, J. S. S. Damsté, and others. 2016. Hydrogen peroxide detoxification is a key mechanism for growth of ammonia-oxidizing archaea. Proc. Natl. Acad. Sci. **113**: 7888–7893. doi:10.1073/pnas.1605501113

Kirk, J. T. O. 1994. Light and Photosynthesis in Aquatic Ecosystems, Cambridge University Press.

Knapp, A. N., D. M. Sigman, and F. Lipschultz. 2005. N isotopic composition of dissolved organic nitrogen and nitrate at the Bermuda Atlantic Time-series Study site. Glob. Biogeochem. Cycles **19**: GB1018. doi:10.1029/2004GB002320

Knapp, A. N., D. M. Sigman, F. Lipschultz, A. B. Kustka, and D. G. Capone. 2011. Interbasin isotopic correspondence between upper-ocean bulk DON and subsurface nitrate and its implications for marine nitrogen cycling. Glob. Biogeochem. Cycles 25: GB4004. doi:10.1029/2010GB003878

Legendre, L., and M. Gosselin. 1997. Estimation of N or C uptake rates by phytoplankton using 15N or 13C: revisiting the usual computation formulae. J. Plankton Res. **19**: 263–271. doi:10.1093/plankt/19.2.263

LeGrande, A. N., and G. A. Schmidt. 2006. Global gridded data set of the oxygen isotopic composition in seawater. Geophys. Res. Lett. **33**: L12604. doi:10.1029/2006GL026011

Letscher, R. T., D. A. Hansell, C. A. Carlson, R. Lumpkin, and A. N. Knapp. 2013. Dissolved organic nitrogen in the global surface ocean: Distribution and fate. Glob. Biogeochem. Cycles 27: 141–153. doi:10.1029/2012GB004449

Lipschultz, F. 2008. Chapter 31 - Isotope Tracer Methods for Studies of the Marine Nitrogen Cycle, p. 1345–1384. *In* Nitrogen in the Marine Environment (2nd Edition). Academic Press.

Lochte, K., H. W. Ducklow, M. J. R. Fasham, and C. Stienen. 1993. Plankton succession and carbon cycling at 47°N 20°W during the JGOFS North Atlantic Bloom Experiment. Deep Sea Res. Part II Top. Stud. Oceanogr. **40**: 91–114. doi:10.1016/0967-0645(93)90008-B

Lomas, M. W., and F. Lipschultz. 2006. Forming the primary nitrite maximum: Nitrifiers or phytoplankton? Limnol. Oceanogr. **51**: 2453–2467. doi:10.4319/lo.2006.51.5.2453

Luo, Y.-W., S. C. Doney, L. A. Anderson, and others. 2012. Database of diazotrophs in global ocean: abundance, biomass and nitrogen fixation rates. Earth Syst. Sci. Data **4**: 47–73. doi:Luo, Y.-W.; Doney, S.C.; Anderson, L.A.; Benavides, M.; Berman-Frank, I.; Bode, A.; Bonnet, S.; Boström, K.H.; Böttjer, D.; Capone, D.G.; Carpenter, E.J.; Chen, Y.L.; Church, M.J.; Dore, J.E.; Falcón, L.I.; Fernández, A.; Foster, R.A.; Furuya, K.; Gómez, F.; Gundersen, K.; Hynes, A.M.; Karl, D.M.; Kitajima, S.; Langlois, R.J.; LaRoche, J.; Letelier, R.M.; Marañón, E.; McGillicuddy, D.J.; Moisander, P.H.; Moore, C.M.; Mouriño-Carballido, B.; Mulholland, M.R.; Needoba, J.A.; Orcutt, K.M.; Poulton, A.J.; Rahav, E.; Raimbault, P.; Rees, A.P.; Riemann, L.; Shiozaki, T.; Subramaniam, A.; Tyrrell, T.; Turk-Kubo, K.A.; Varela, M.; Villareal, T.A.; Webb, E.A.; White, A.E.; Wu, J.; Zehr, J.P.. 2012 Database of diazotrophs in global ocean: abundance, biomass and nitrogen fixation rates. Earth System Science Data, 4 (1). 47-73. 10.5194/essd-4-47-2012 <http://dx.doi.org/10.5194/essd-4-47-2012>

Marconi, D., M. Alexandra Weigand, P. A. Rafter, M. R. McIlvin, M. Forbes, K. L. Casciotti, and D. M. Sigman. 2015. Nitrate isotope distributions on the US GEOTRACES North Atlantic cross-basin section: Signals of polar nitrate sources and low latitude nitrogen cycling. Mar. Chem. **177**, **Part 1**: 143–156. doi:10.1016/j.marchem.2015.06.007

Marconi, D., S. Kopf, P. A. Rafter, and D. M. Sigman. 2017. Aerobic respiration along isopycnals leads to overestimation of the isotope effect of denitrification in the ocean water column. Geochim. Cosmochim. Acta **197**: 417–432. doi:10.1016/j.gca.2016.10.012

Martens-Habbena, W., W. Qin, R. E. A. Horak, H. Urakawa, A. J. Schauer, J. W. Moffett, E. V. Armbrust, A. E. Ingalls, A. H. Devol, and D. A. Stahl. 2015. The production of nitric oxide by marine ammonia-oxidizing archaea and inhibition of archaeal ammonia oxidation by a nitric oxide scavenger. Environ. Microbiol. **17**: 2261–2274. doi:10.1111/1462-2920.12677

Martin, A. P., and P. Pondaven. 2006. New primary production and nitrification in the western subtropical North Atlantic: A modeling study. Glob. Biogeochem. Cycles **20**: GB4014. doi:10.1029/2005GB002608

Martin-Jézéquel, V., M. Hildebrand, and M. A. Brzezinski. 2000. Silicon Metabolism in Diatoms: Implications for Growth. J. Phycol. **36**: 821–840. doi:10.1046/j.1529-8817.2000.00019.x

McIlvin, M. R., and M. A. Altabet. 2005. Chemical Conversion of Nitrate and Nitrite to Nitrous Oxide for Nitrogen and Oxygen Isotopic Analysis in Freshwater and Seawater. Anal. Chem. **77**: 5589–5595. doi:10.1021/ac050528s

McIlvin, M. R., and K. L. Casciotti. 2011. Technical Updates to the Bacterial Method for Nitrate Isotopic Analyses. Anal. Chem. **83**: 1850–1856. doi:10.1021/ac1028984

Merbt, S. N., D. A. Stahl, E. O. Casamayor, E. Martí, G. W. Nicol, and J. I. Prosser. 2012. Differential photoinhibition of bacterial and archaeal ammonia oxidation. FEMS Microbiol. Lett. **327**: 41–46. doi:10.1111/j.1574-6968.2011.02457.x

Möbius, J. 2013. Isotope fractionation during nitrogen remineralization (ammonification): Implications for nitrogen isotope biogeochemistry. Geochim. Cosmochim. Acta **105**: 422–432. doi:10.1016/j.gca.2012.11.048

Moore, C. M., M. M. Mills, K. R. Arrigo, and others. 2013. Processes and patterns of oceanic nutrient limitation. Nat. Geosci. **6**: 701–710. doi:10.1038/ngeo1765

NASA Goddard Space Flight Center, Ocean Ecology Laboratory, Ocean Biology Processing Group. Moderate-resolution Imaging Spectroradiometer (MODIS) Aqua Chlorophyll Data; 2013 and 2014 Reprocessing. NASA OB.DAAC, Greenbelt, MD, USA. doi:10.5067/AQUA/MODIS/L3M/CHL/2013 and doi:10.5067/AQUA/MODIS/L3M/CHL/2014

Newell, S. E., S. E. Fawcett, and B. B. Ward. 2013. Depth distribution of ammonia oxidation rates and ammonia-oxidizer community composition in the Sargasso Sea. Limnol. Oceanogr. **58**: 1491–1500. doi:10.4319/lo.2013.58.4.1491

Nielsdóttir, M. C., C. M. Moore, R. Sanders, D. J. Hinz, and E. P. Achterberg. 2009. Iron limitation of the postbloom phytoplankton communities in the Iceland Basin. Glob. Biogeochem. Cycles **23**: GB3001. doi:10.1029/2008GB003410

Olson, R. J. 1981. Differential photoinhibition of marine nitrifying bacteria: a possible mechanism for the formation of the primary nitrite maximum. J. Mar. Res **39**: 227–238.

Owens, N. J. P., J. N. Galloway, and Duce. 1992. Episodic atmospheric nitrogen deposition to oligotrophic oceans. Nature **357**: 397–399. doi:10.1038/357397a0

Paerl, H. W. 1991. Ecophysiological and Trophic Implications of Light-Stimulated Amino Acid Utilization in Marine Picoplankton. Appl. Environ. Microbiol. **57**: 473–479.

Peng, X., C. A. Fuchsman, A. Jayakumar, S. Oleynik, W. Martens-Habbena, A. H. Devol, and B. B. Ward. 2015. Ammonia and nitrite oxidation in the Eastern Tropical North Pacific. Glob. Biogeochem. Cycles **29**: 2015GB005278. doi:10.1002/2015GB005278

Peng, X., C. A. Fuchsman, A. Jayakumar, M. J. Warner, A. H. Devol, and B. B. Ward. 2016. Revisiting nitrification in the Eastern Tropical South Pacific: A focus on controls. J. Geophys. Res. Oceans **121**: 1667–1684. doi:10.1002/2015JC011455

Qi, H., T. B. Coplen, H. Geilmann, W. A. Brand, and J. K. Böhlke. 2003. Two new organic reference materials for δ13C and δ15N measurements and a new value for the δ13C

of NBS 22 oil. Rapid Commun. Mass Spectrom. **17**: 2483–2487. doi:10.1002/rcm.1219

Qin, W., S. A. Amin, W. Martens-Habbena, and others. 2014. Marine ammonia-oxidizing archaeal isolates display obligate mixotrophy and wide ecotypic variation. Proc. Natl. Acad. Sci. **111**: 12504–12509. doi:10.1073/pnas.1324115111

Rafter, P. A., and D. M. Sigman. 2016. Spatial distribution and temporal variation of nitrate nitrogen and oxygen isotopes in the upper equatorial Pacific Ocean. Limnol. Oceanogr. 61: 14–31. doi:10.1002/lno.10152

Raimbault, P., and N. Garcia. 2008. Evidence for efficient regenerated production and dinitrogen fixation in nitrogen-deficient waters of the South Pacific Ocean: impact on new and export production estimates. Biogeosciences **5**: 323–338. doi:10.5194/bg-5-323-2008

Raimbault, P., G. Slawyk, B. Boudjellal, and others. 1999. Carbon and nitrogen uptake and export in the equatorial Pacific at 150°W: Evidence of an efficient regenerated production cycle. J. Geophys. Res. Oceans **104**: 3341–3356. doi:10.1029/1998JC900004

Riegman, R., and A. A. M. Noordeloos. 1998. Size-fractionated uptake of nitrogenous nutrients and carbon by phytoplankton in the North Sea during summer 1994. Mar. Ecol. Prog. Ser. **173**: 95–106. doi:10.3354/meps173095

Rohde, M. M., J. Granger, D. M. Sigman, and M. F. Lehmann. 2015. Coupled nitrate N and O stable isotope fractionation by a natural marine plankton consortium. Front. Mar. Sci. 2. doi:10.3389/fmars.2015.00028

Rynearson, T. A., K. Richardson, R. S. Lampitt, M. E. Sieracki, A. J. Poulton, M. M. Lyngsgaard, and M. J. Perry. 2013. Major contribution of diatom resting spores to vertical flux in the sub-polar North Atlantic. Deep-Sea Res. I **82**: 60–71. doi:Rynearson, T.A., Richardson, K., Lampitt, R.S., Sieracki, M.E., Poulton, A.J., Lyngsgaard, M.M. and Perry, M.J. (2013) Major contribution of diatom resting spores to vertical flux in the sub-polar North Atlantic Deep-Sea Research I, 82, pp. 60-71. (doi:10.1016/j.dsr.2013.07.013 <http://dx.doi.org/10.1016/j.dsr.2013.07.013>).

Saito, M. A., M. R. McIlvin, D. M. Moran, T. J. Goepfert, G. R. DiTullio, A. F. Post, and C. H. Lamborg. 2014. Multiple nutrient stresses at intersecting Pacific Ocean biomes detected by protein biomarkers. Science **345**: 1173–1177. doi:10.1126/science.1256450

Santoro, A. E., K. L. Casciotti, and C. A. Francis. 2010. Activity, abundance and diversity of nitrifying archaea and bacteria in the central California Current. Environ. Microbiol. **12**: 1989–2006. doi:10.1111/j.1462-2920.2010.02205.x

Santoro, A. E., C. L. Dupont, R. A. Richter, and others. 2015. Genomic and proteomic characterization of "Candidatus Nitrosopelagicus brevis": An ammonia-oxidizing archaeon from the open ocean. Proc. Natl. Acad. Sci. **112**: 1173–1178. doi:10.1073/pnas.1416223112

Santoro, A. E., C. M. Sakamoto, J. M. Smith, and others. 2013. Measurements of nitrite production in and around the primary nitrite maximum in the central California Current. Biogeosciences **10**: 7395–7410. doi:10.5194/bg-10-7395-2013

Schön, G. H., and H. Engel. 1962. Der Einfluß des Lichtes auf Nitrosomonas europaea Win. Arch. Für Mikrobiol. **42**: 415–428. doi:10.1007/BF00409076

Shiozaki, T., M. Ijichi, K. Isobe, and others. 2016. Nitrification and its influence on biogeochemical cycles from the equatorial Pacific to the Arctic Ocean. ISME J. **10**: 2184–2197. doi:10.1038/ismej.2016.18

Sigman, D. M., M. A. Altabet, D. C. McCorkle, R. Francois, and G. Fischer. 1999. The δ15N of nitrate in the southern ocean: Consumption of nitrate in surface waters. Glob. Biogeochem. Cycles **13**: 1149–1166. doi:10.1029/1999GB900038

Sigman, D. M., K. L. Casciotti, M. Andreani, C. Barford, M. Galanter, and J. K. Böhlke. 2001. A Bacterial Method for the Nitrogen Isotopic Analysis of Nitrate in Seawater and Freshwater. Anal. Chem. **73**: 4145–4153. doi:10.1021/ac010088e

Sigman, D. M., J. Granger, P. J. DiFiore, M. M. Lehmann, R. Ho, G. Cane, and A. van Geen. 2005. Coupled nitrogen and oxygen isotope measurements of nitrate along the eastern North Pacific margin. Glob. Biogeochem. Cycles **19**: GB4022. doi:10.1029/2005GB002458

Sigman, D. M., P. J. DiFiore, M. P. Hain, and others. 2009a. The dual isotopes of deep nitrate as a constraint on the cycle and budget of oceanic fixed nitrogen. Deep Sea Res. Part Oceanogr. Res. Pap. 56: 1419–1439. doi:10.1016/j.dsr.2009.04.007

Sigman, D. M., K. L. Karsh, and K. L. Casciotti. 2009b. Ocean process tracers: nitrogen isotopes in the ocean.

Smart, S. M., S. E. Fawcett, S. J. Thomalla, M. A. Weigand, C. J. C. Reason, and D. M. Sigman. 2015. Isotopic evidence for nitrification in the Antarctic winter mixed layer. Glob. Biogeochem. Cycles **29**: 2014GB005013. doi:10.1002/2014GB005013

Smith, J. M., F. P. Chavez, and C. A. Francis. 2014. Ammonium Uptake by Phytoplankton Regulates Nitrification in the Sunlit Ocean. PLOS ONE **9**: e108173. doi:10.1371/journal.pone.0108173

Spokes, L. J., S. G. Yeatman, S. E. Cornell, and T. D. Jickells. 2000. Nitrogen deposition to the eastern Atlantic Ocean. The importance of south-easterly flow. Tellus B **52**: 37–49. doi:10.1034/j.1600-0889.2000.00062.x

Strickland, J. D. H., and T. R. Parsons. 1972. A Practical Handbook of Seawater Analysis, Fisheries Research Board of Canada.

Stukel, M. R., C. R. Benitez-Nelson, M. Décima, A. G. Taylor, C. Buchwald, and M. R. Landry. 2016. The biological pump in the Costa Rica Dome: an open-ocean upwelling system with high new production and low export. J. Plankton Res. **38**: 348–365. doi:10.1093/plankt/fbv097

Sutka, R. L., N. E. Ostrom, P. H. Ostrom, and M. S. Phanikumar. 2004. Stable nitrogen isotope dynamics of dissolved nitrate in a transect from the north Pacific subtropical gyre to the eastern tropical north Pacific 1. Geochim. Cosmochim. Acta **68**: 517–527. doi:10.1016/S0016-7037(03)00483-6

Tarran, G. A., M. V. Zubkov, M. A. Sleigh, P. H. Burkill, and M. Yallop. 2001. Microbial community structure and standing stocks in the NE Atlantic in June and July of 1996. Deep-Sea Res. II **48**: 963–985. doi:Tarran, G.A.; Zubkov, M.V.; Sleigh, M.A.; Burkill, P.H.; Yallop, M.. 2001 Microbial community structure and standing stocks in the NE Atlantic in June and July of 1996. Deep-Sea Research II, 48 (4-5). 963-985. 10.1016/S0967-0645(00)00104-1 <http://dx.doi.org/10.1016/S0967-0645(00)00104-1>

Thompson, P. A., M. E. Levasseur, and P. J. Harrison. 1989. Light-limited growth on ammonium vs. nitrate: What is the advantage for marine phytoplankton? Limnol. Oceanogr. **34**: 1014–1024. doi:10.4319/lo.1989.34.6.1014

Tolar, B. B., L. C. Powers, W. L. Miller, N. J. Wallsgrove, B. N. Popp, and J. T. Hollibaugh. 2016. Ammonia Oxidation in the Ocean Can Be Inhibited by Nanomolar Concentrations of Hydrogen Peroxide. Front. Mar. Sci. **3**. doi:10.3389/fmars.2016.00237

Trull, T. W., D. Davies, and K. Casciotti. 2008. Insights into nutrient assimilation and export in naturally iron-fertilized waters of the Southern Ocean from nitrogen, carbon and

oxygen isotopes. Deep Sea Res. Part II Top. Stud. Oceanogr. 55: 820–840. doi:10.1016/j.dsr2.2007.12.035

Van Oostende, N., S. E. Fawcett, D. Marconi, and others. 2017. Variation of summer phytoplankton community composition and its relationship to nitrate and regenerated nitrogen assimilation across the North Atlantic Ocean. Deep Sea Res. Part I **121**: 79–94.

Varela, M. M., A. Bode, E. Fernández, N. Gónzalez, V. Kitidis, M. Varela, and E. M. S. Woodward. 2005. Nitrogen uptake and dissolved organic nitrogen release in planktonic communities characterised by phytoplankton size–structure in the Central Atlantic Ocean. Deep Sea Res. Part Oceanogr. Res. Pap. **52**: 1637–1661. doi:10.1016/j.dsr.2005.03.005

Wada, E., and A. Hattori. 1978. Nitrogen isotope effects in the assimilation of inorganic nitrogenous compounds by marine diatoms. Geomicrobiol. J. **1**: 85–101. doi:10.1080/01490457809377725

Walker, C. B., J. R. de la Torre, M. G. Klotz, and others. 2010. Nitrosopumilus maritimus genome reveals unique mechanisms for nitrification and autotrophy in globally distributed marine crenarchaea. Proc. Natl. Acad. Sci. **107**: 8818–8823. doi:10.1073/pnas.0913533107

Wankel, S. D., C. Kendall, J. T. Pennington, F. P. Chavez, and A. Paytan. 2007. Nitrification in the euphotic zone as evidenced by nitrate dual isotopic composition: Observations from Monterey Bay, California. Glob. Biogeochem. Cycles **21**: GB2009. doi:10.1029/2006GB002723

Ward, B. B. 1985. Light and substrate concentration relationships with marine ammonium assimilation and oxidation rates. Mar. Chem. **16**: 301–316. doi:10.1016/0304-4203(85)90052-0

Ward, B. B. 2005. Temporal variability in nitrification rates and related biogeochemical factors in Monterey Bay, California, USA. Mar. Ecol. Prog. Ser. **292**: 97–109. doi:10.3354/meps292097

Ward, B. B. 2011. Nitrification in the Ocean. Nitrification 325–345. doi:10.1128/9781555817145.ch13

Ward, B. B., H. E. Glover, and F. Lipschultz. 1989. Chemoautotrophic activity and nitrification in the oxygen minimum zone off Peru. Deep Sea Res. Part Oceanogr. Res. Pap. **36**: 1031–1051. doi:10.1016/0198-0149(89)90076-9

Ward, B. B., and O. C. Zafiriou. 1988. Nitrification and nitric oxide in the oxygen minimum of the eastern tropical North Pacific. Deep Sea Res. A **35**: 1127–1142. doi:10.1016/0198-0149(88)90005-2

Ward, B.B., Allen, A.E., and Sigman, D.M. 2016. Dissolved inorganic nutrient concentrations from ctd cast deployments and underway seawater inflow from Endeavor 532 and Endeavor 538. Biological and Chemical Oceanography Data Management Office (BCO-DMO). Dataset version 2016-07-14. http://lod.bco-dmo.org/id/dataset/651816

Weigand, M. A., J. Foriel, B. Barnett, S. Oleynik, and D. M. Sigman. 2016. Updates to instrumentation and protocols for isotopic analysis of nitrate by the denitrifier method. Rapid Commun. Mass Spectrom. **30**: 1365–1383. doi:10.1002/rcm.7570

Wheeler, P. A., and S. A. Kokkinakis. 1990. Ammonium recycling limits nitrate use in the oceanic subarctic Pacific. Limnol. Oceanogr. **35**: 1267–1278. doi:10.4319/lo.1990.35.6.1267

Woodward, E. M. S., and A. P. Rees. 2001. Nutrient distributions in an anticyclonic eddy in the northeast Atlantic Ocean, with reference to nanomolar ammonium concentrations.

Deep Sea Res. Part II Top. Stud. Oceanogr. **48**: 775–793. doi:10.1016/S0967-0645(00)00097-7

Yool, A., A. P. Martin, C. Fernández, and D. R. Clark. 2007. The significance of nitrification for oceanic new production. Nature **447**: 999–1002. doi:10.1038/nature05885

Zunino, P., P. Lherminier, H. Mercier, X. A. Padín, A. F. Ríos, and F. F. Pérez. 2015. Dissolved inorganic carbon budgets in the eastern subpolar North Atlantic in the 2000s from in situ data. Geophys. Res. Lett. **42**: 2015GL066243. doi:10.1002/2015GL066243

Table 1: Euphotic zone integrated rates of NH_4^+ and NO_3^- uptake (ρ_{NH4_integ} and ρ_{NO3_integ}), NH_4^+ and NO_2^- oxidation (V_{NH4_integ} and V_{NO2_integ}), the percentage (%) of NH_4^+ and NO_2^- oxidation relative to NO_3^- uptake ($V_{NH4\_integ}/\rho_{NO3\_integ}$ and $V_{NO2\_integ}/\rho_{NO3\_integ}$), and the concentration of total particulate organic nitrogen (PON_{integ}) and carbon (POC_{integ}). Also shown is the depth-weighted average euphotic zone f-ratio ($(\rho_{NO3}/(\rho_{NO3} + \rho_{NH4}))$, the euphotic zone integrated rate of NH_4^+ oxidation relative to NO_2^- oxidation ($V_{NH4\_integ}/V_{NO2\_integ}$), and regenerated production relative to NH_4^+ oxidation ($\rho_{NH4\_integ}/V_{NH4\_integ}$) (i.e., $V_{NH4\_integ}/V_{NO2\_integ}$ = 5.1 indicates that the euphotic zone integrated rate of NH_4^+ oxidation is 5.1 times that of NO_2^- oxidation, and $\rho_{NH4\_integ}/V_{NH4\_integ}$ = 34 indicates that the euphotic zone integrated rate of NH_4^+ uptake is 34 times that of NH_4^+ oxidation). For EN538 PS2, the values in parentheses are those calculated assuming a euphotic zone depth of 82 m (i.e., 0.1% PAR) since significant rates of NO_3^- and NH_4^+ uptake were measured at this depth (Figure 4).

	September		May	
	EN532 PS1	EN532 PS2	EN538 PS1	EN538 PS2
latitude °N; longitude °W	54.00; 20.00	50.00; 20.00	58.00; 20.00	59.50; 21.35
Euphotic zone depth (m)	51	42	51	57 (82)
Mixed layer depth (m)	50	40	40	55
Sampling depths (m) for N uptake and NPP experiments	15, 25, 50	15, 23, 35	25, 45, 50	20, 40, 82
Sampling depths (m) for nitrification experiments	20, 40, 50, 60, 100, 250, 500	20, 40, 50, 60, 100, 250, 500	25, 37, 60, 80, 100, 300, 1000	50, 80, 90, 100, 125, 250, 1000
PON_{integ} (mmol m^{-2})	81.9	71.5	81.8	103.0 (115.9)
POC_{integ} (mmol m^{-2})	502.9	450.5	540.7	631.4 (710.5)
ρ_{NH4_integ} (µmol m^{-2} d^{-1})	2225	3265	2549	4526 (5408)
ρ_{NO3_integ} (µmol m^{-2} d^{-1})	3614	837	1629	2993 (3482)
V_{NH4_integ} (µmol m^{-2} d^{-1})	66.4	91.2	113.0	31.0 (570.0)
V_{NO2_integ} (µmol m^{-2} d^{-1})	13.0	43.0	25.7	86.8 (213.3)
$V_{NH4\_integ}/\rho_{NO3\_integ}$ (%)	1.84	10.9	6.94	1.04 (16.4)
$V_{NO2\_integ}/\rho_{NO3\_integ}$ (%)	0.36	5.14	1.58	2.90 (6.13)
f-ratio	0.62	0.20	0.39	0.40 (0.39)
$V_{NH4\_integ}/V_{NO2\_integ}$	5.1	2.1	4.4	0.36 (2.7)
$\rho_{NH4\_integ}/V_{NH4\_integ}$	34	36	23	146 (9.5)

Table 2: Weighted average euphotic zone biomass C:N ratio (i.e., POC_{integ}/PON_{integ}), and euphotic zone integrated rates of ^{13}C-based NPP, ^{15}N-based $NO_3^-+NH_4^+$ uptake (i.e., N uptake), and NPP calculated from N uptake multiplied by the measured biomass C:N ratio. Because only one incubation experiment could be performed each day (Figure 2), there were likely fluctuations in water column density structure at the same station (see text); however, each set of NPP and N uptake incubations from a particular depth were performed concomitantly.

Month and Station	Average Biomass C:N	Integrated NPP (mmol m^{-2} d^{-1})	Integrated N uptake ($\rho_{NO3}+\rho_{NH4}$) (mmol m^{-2} d^{-1})	Integrated NPP (N uptake x C:N) (mmol m^{-2} d^{-1})
Sept. PS1	6.14	77.2	5.84	35.9
Sept. PS2	6.30	49.1	4.10	25.8
May PS1	6.61	27.4	4.18	27.6
May PS2	6.13	46.5	7.52	46.1

Figure captions

Figure 1: Location of the process stations (PS) sampled in September 2013 (EN532, left panel) and May 2014 (EN538, right panel) in the subarctic North Atlantic. Monthly climatological surface NO_3^- concentrations (μmol l^{-1}) are shown with color contours (World Ocean Atlas 2013, Garcia et al. 2013).

Figure 2: Mixed layer depth (MLD, red solid line) and euphotic zone depth defined by the depth of 1% of surface photosynthetically active radiation (1% PAR, blue dashed line) over the course of the four- to five-day occupation at each process station (PS). Depth profiles of NO_3^- concentration (μmol l^{-1}) are overlaid as colored circles, ranging from below detection (blue) to 12 μmol l^{-1} (yellow). The sampling depths and times are marked with gray crosses for the N uptake and NPP incubations and black crosses for nitrification incubations.

Figure 3: Depth profiles of NH_4^+ concentration (μmol l^{-1}), NO_2^- concentration (μmol l^{-1}), NO_3^- concentration (μmol l^{-1}), NH_4^+ and NO_3^- uptake rates (nmol l^{-1} d^{-1}), NPP (nmol l^{-1} d^{-1}) and POC concentration (μmol l^{-1}), and NH_4^+ and NO_2^- oxidation rates (nmol l^{-1} d^{-1}) at process stations (PS) 1 and 2 in late summer (September 2013). For NH_4^+, NO_2^-, and NO_3^- concentrations, the filled symbols indicate measurements made from the casts used to collect seawater for the NH_4^+ and NO_2^- oxidation incubations, and the hollow symbols represent measurements from all other casts at the same station.

Figure 4: Depth profiles of NH_4^+ concentration (μmol l^{-1}), NO_2^- concentration (μmol l^{-1}), NO_3^- concentration (μmol l^{-1}), NH_4^+ and NO_3^- uptake rates (nmol l^{-1} d^{-1}), NPP (nmol l^{-1} d^{-1}) and POC concentration (μmol l^{-1}), and NH_4^+ and NO_2^- oxidation rates (nmol l^{-1} d^{-1}) at process stations (PS) 1 and 2 in late spring (May 2014). For NH_4^+, NO_2^-, and NO_3^- concentrations, the filled symbols indicate measurements made from the casts used to collect seawater for the NH_4^+ and NO_2^- oxidation incubations, and the hollow symbols represent measurements from all other casts at the same station.

Figure 5: Vertical profiles (0-1000 m) for September of A) NO_3^- $\delta^{15}N$ and B) NO_3^- $\delta^{18}O$ and for May of C) NO_3^- $\delta^{15}N$ and D) NO_3^- $\delta^{18}O$ (0-1000 m) measured at the process stations, with open symbols for PS1 and filled symbols for PS2. The black symbols show the isotopic composition of NO_3^--only (after NO_2^- removal) and the grey symbols show the isotopes of

NO_3^-+NO_2^-. Error bars indicate ± 1 S.D. (n ≥ 3); where error bars are not present, they are smaller than the data markers.

Figure 6: Upper ocean (0-200 m) profiles of A) NO_2^- concentration (μmol l^{-1}) and B) calculated NO_2^- $\delta^{15}N$ for all samples with NO_2^- concentrations ≥0.1 μmol l^{-1}. In panel B, the color shading denotes the percentage of NO_2^- measured in the samples relative to the NO_3^- +NO_2^- concentration (%NO_2^-). Error bars indicate the standard deviation of the 100,000 Monte Carlo iterations run for each sample.

Figure 7: A compilation of data showing the contribution of nitrification to NO_3^- uptake by phytoplankton, integrated over the euphotic zone or mixed layer, versus the concurrently-measured rate of primary production. The cited studies include Raimb08 (Raimbault and Garcia 2008), Santo10 (Santoro et al. 2010), Beman12 (Beman et al. 2012), Cavag15 (Cavagna et al. 2015), Clark16 (Clark et al. 2016), Shioz16 (Shiozaki et al. 2016), and Stuke16 (Stukel et al. 2016).

Figure 8: Cross plots of NO_3^- $\delta^{18}O$ vs. $\delta^{15}N$ for samples collected between 500 m and the surface in A) September at PS1, B) September at PS2, C) May at PS1, and D) May at PS2. The NO_3^-+NO_2^- samples are shown in grey and the NO_3^--only samples are shown in color, where the color indicates sample depth. The trend lines (dashed grey for NO_3^-+NO_2^- and solid black for NO_3^--only) indicate the ratio of the change in $\delta^{18}O$ relative to $\delta^{15}N$ ($\Delta\delta^{18}O$:$\Delta\delta^{15}N$) for samples collected above 100 m in September and 150 m in May, with the value of the slope indicated on the figure panels. For the NO_3^-+NO_2^- data from PS2 in September, there is no linear relationship between $\delta^{18}O$ and $\delta^{15}N$, likely because the concentration of NO_2^- relative to NO_3^-+NO_2^- was high in surface waters at this station (≥ 8%); this has been shown to significantly alter the relationship between the N and O isotopes of the combined NO_3^- +NO_2^- pool (Fawcett et al., 2015). Note the differences in axis scale between panels A and C and panels B and D.

Figure 9: Cross plot showing total euphotic zone integrated carbon fixation (i.e., net primary production; NPP), as implied by the summed rate of NO_3^-+NH_4^+ uptake multiplied by the measured biomass C:N ratio, versus ^{13}C-based measurements of NPP, also integrated over

the euphotic zone. The dashed line indicates a relationship of 1:1, which is expected if the total rate of NPP can be accounted for by NO_3^- and NH_4^+ uptake only.

Figure 1:

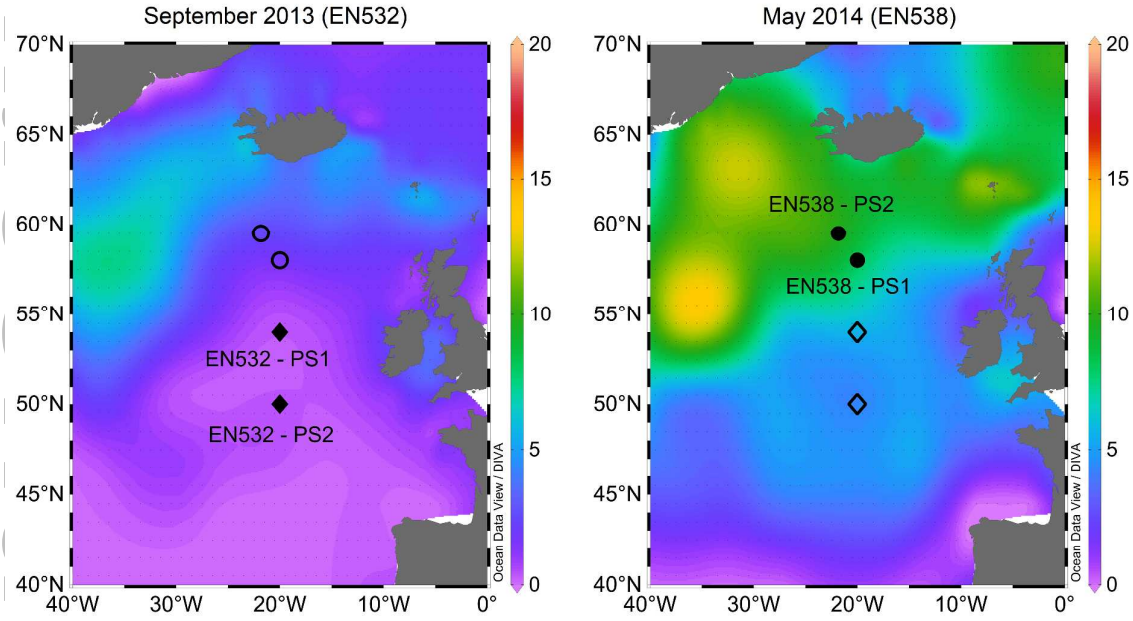

Figure 2:

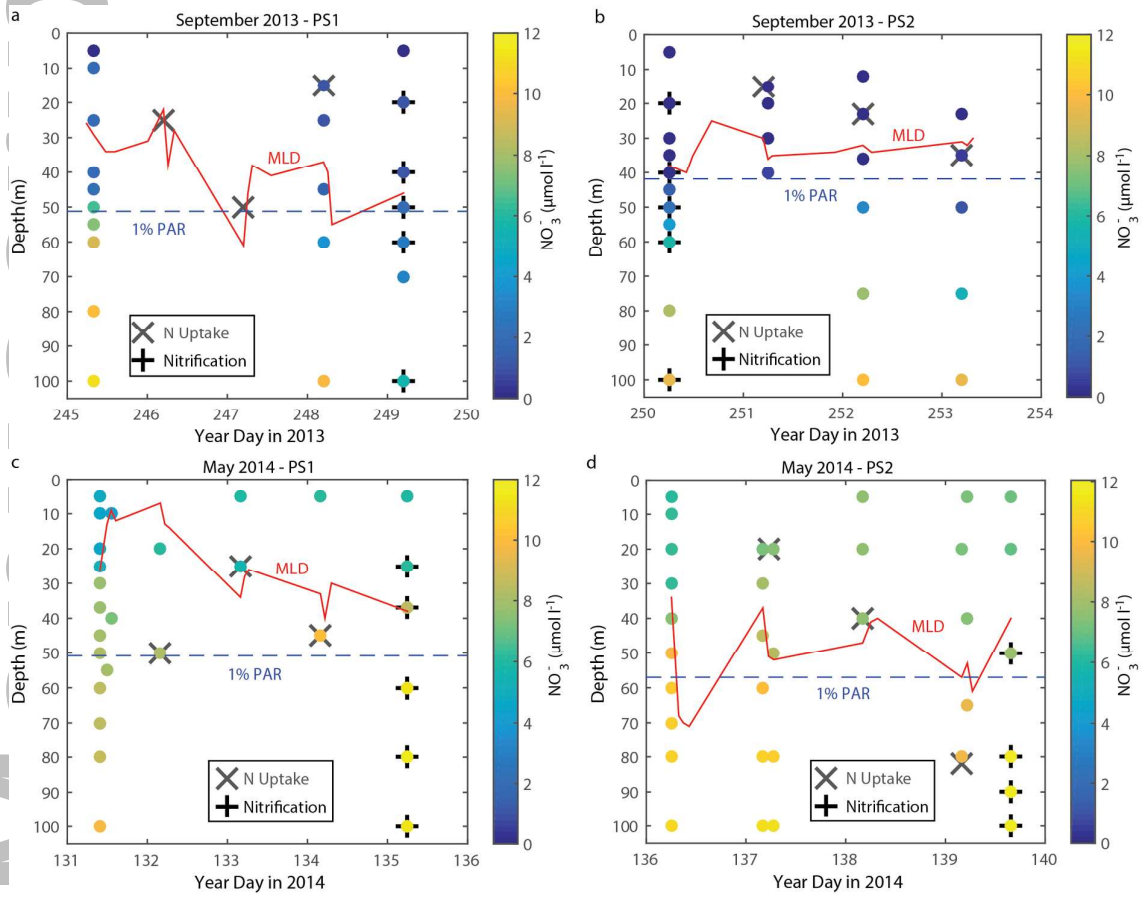

Figure 3:

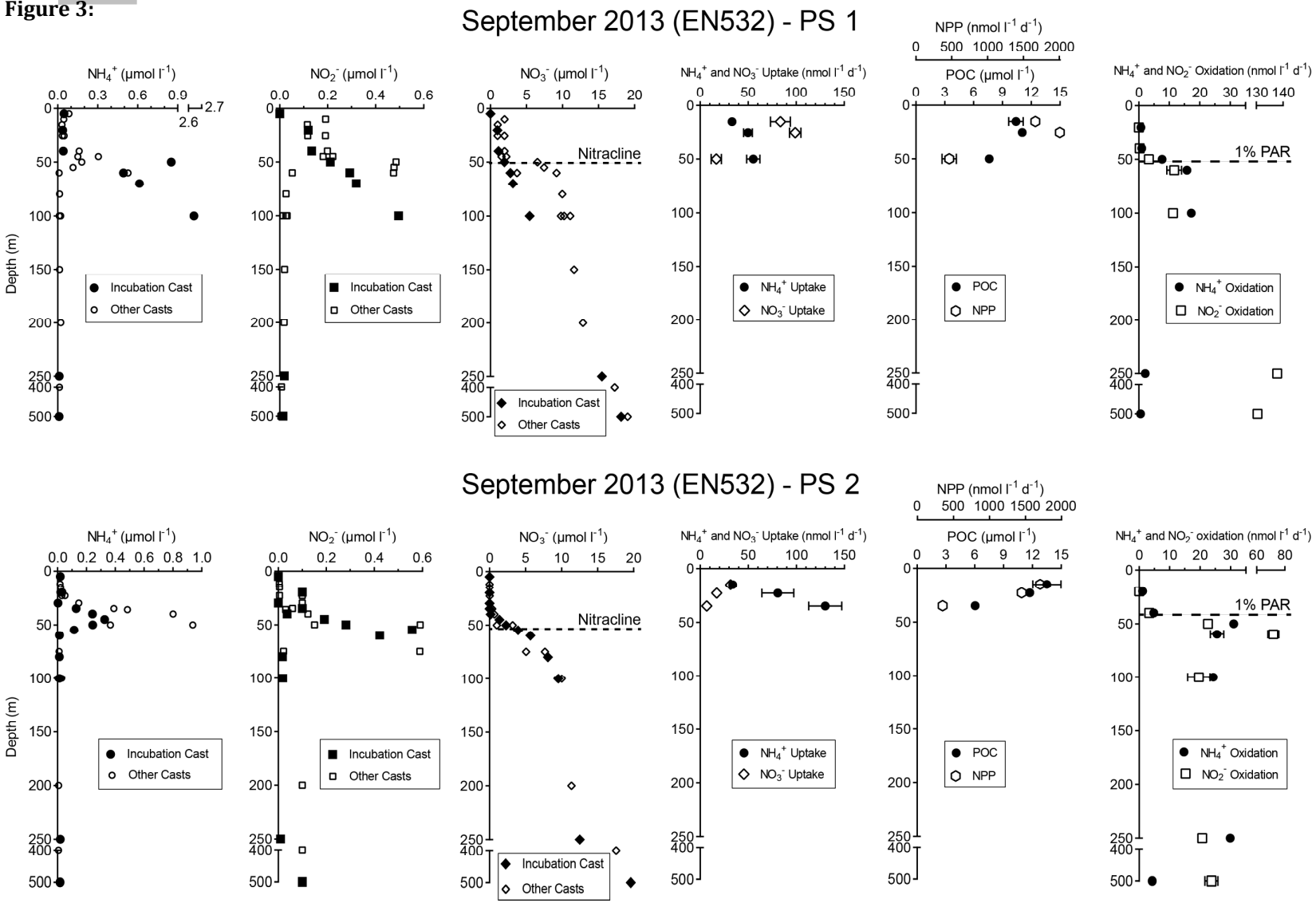

Figure 4:

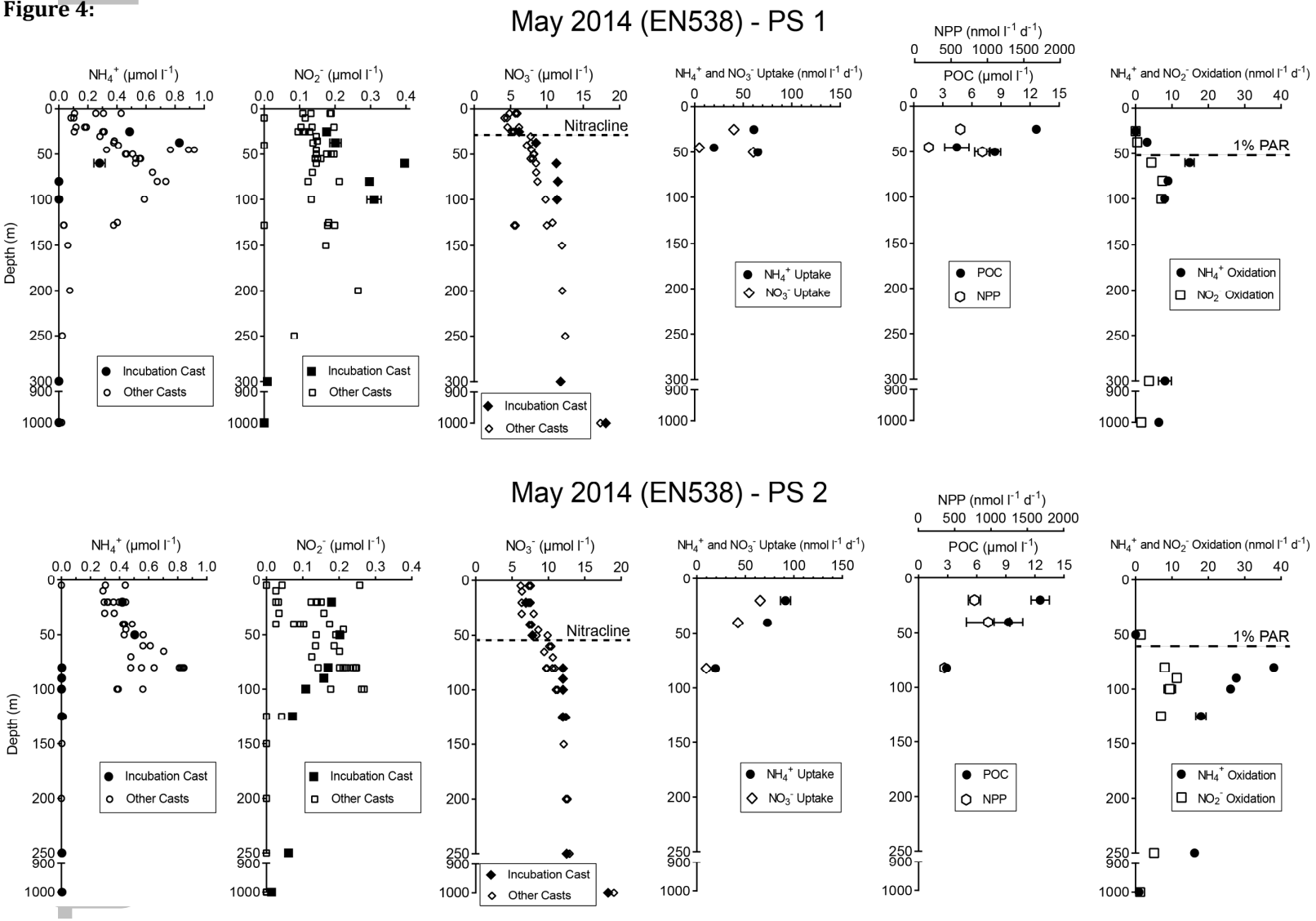

Figure 5:

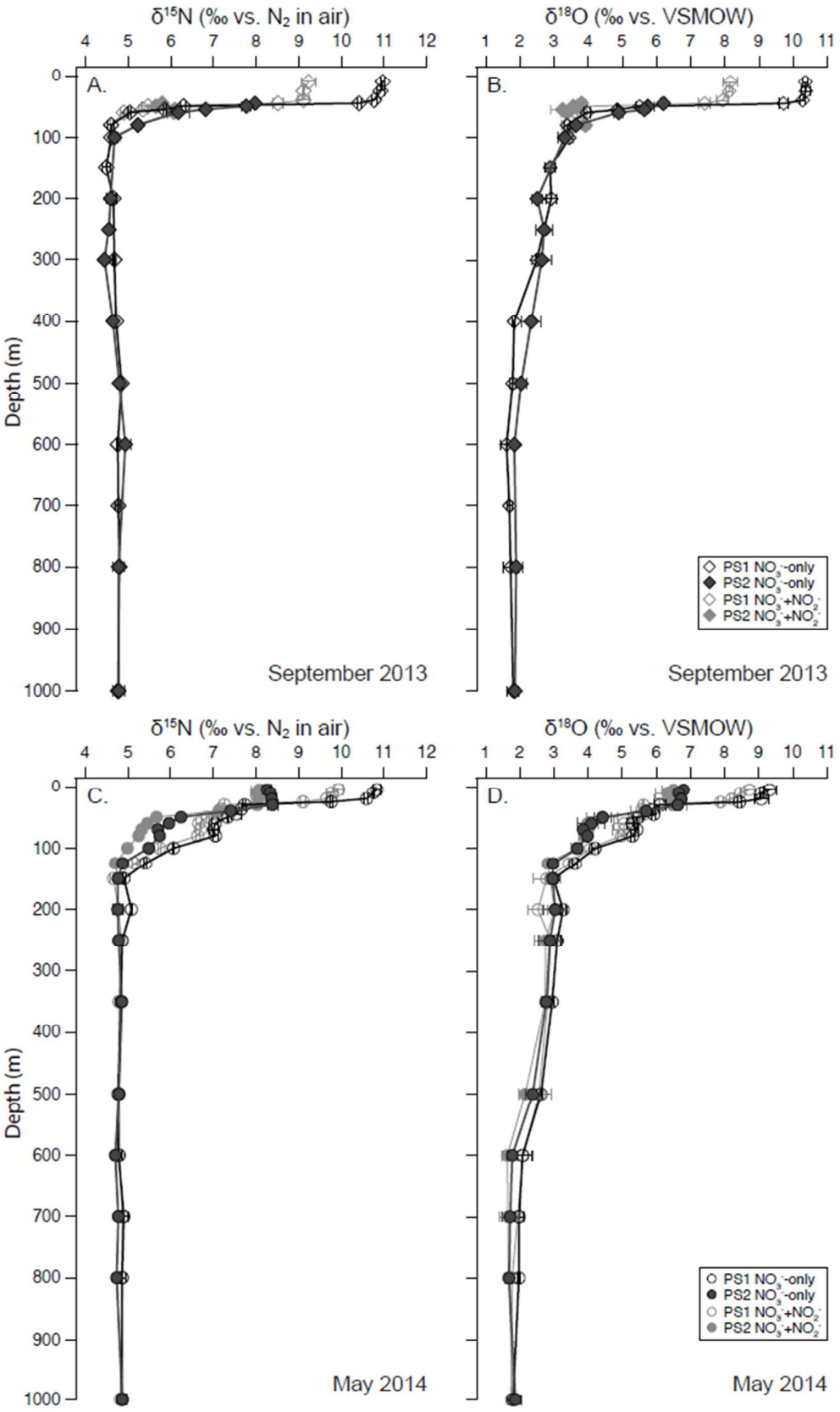

Figure 6:

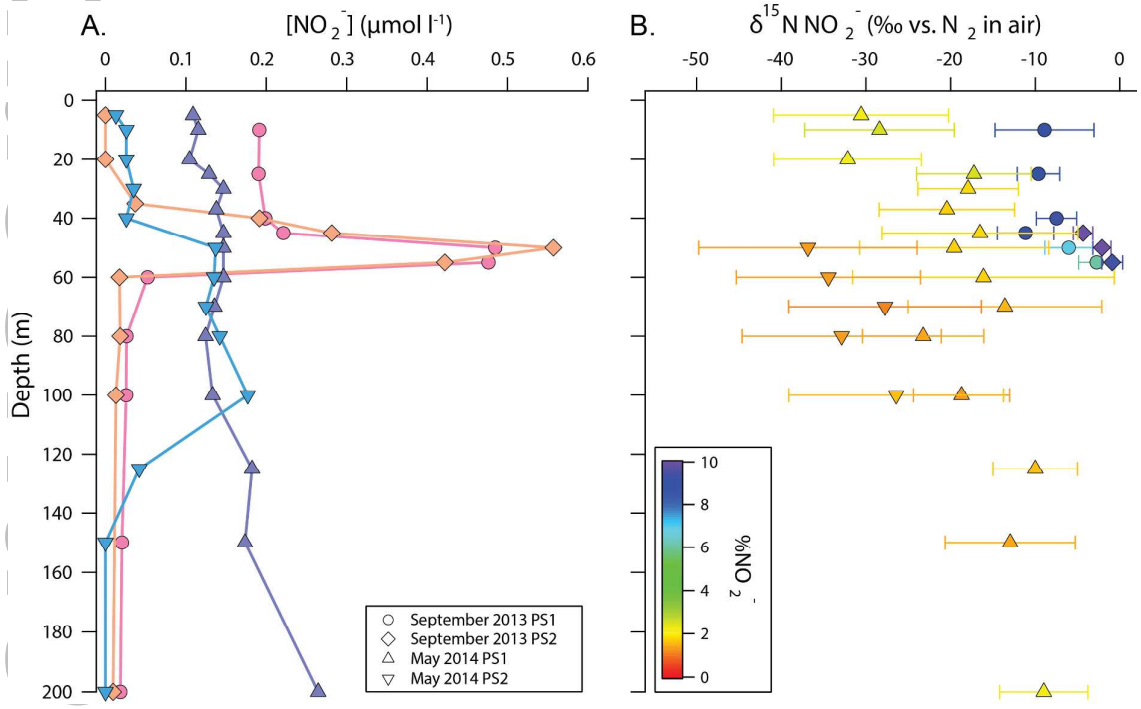

Figure 7:

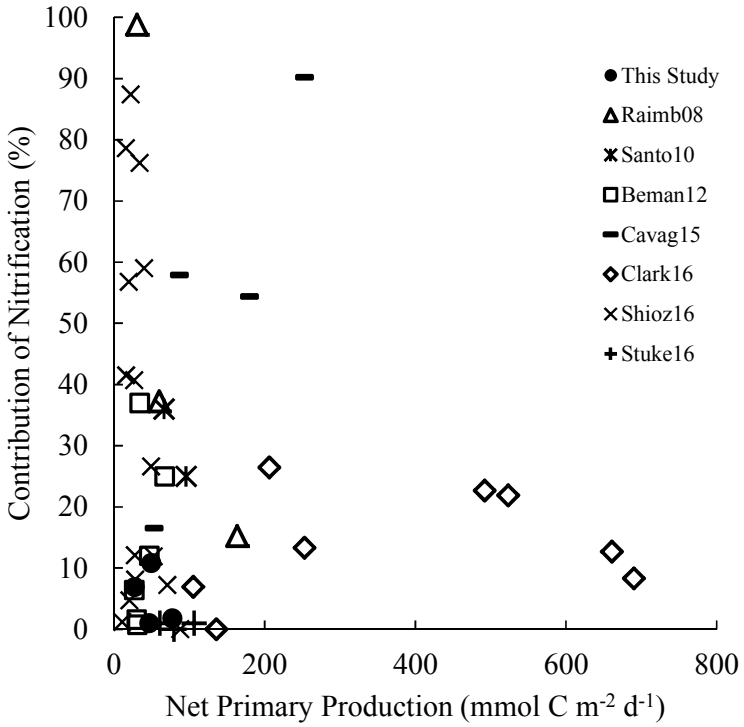

Figure 8:

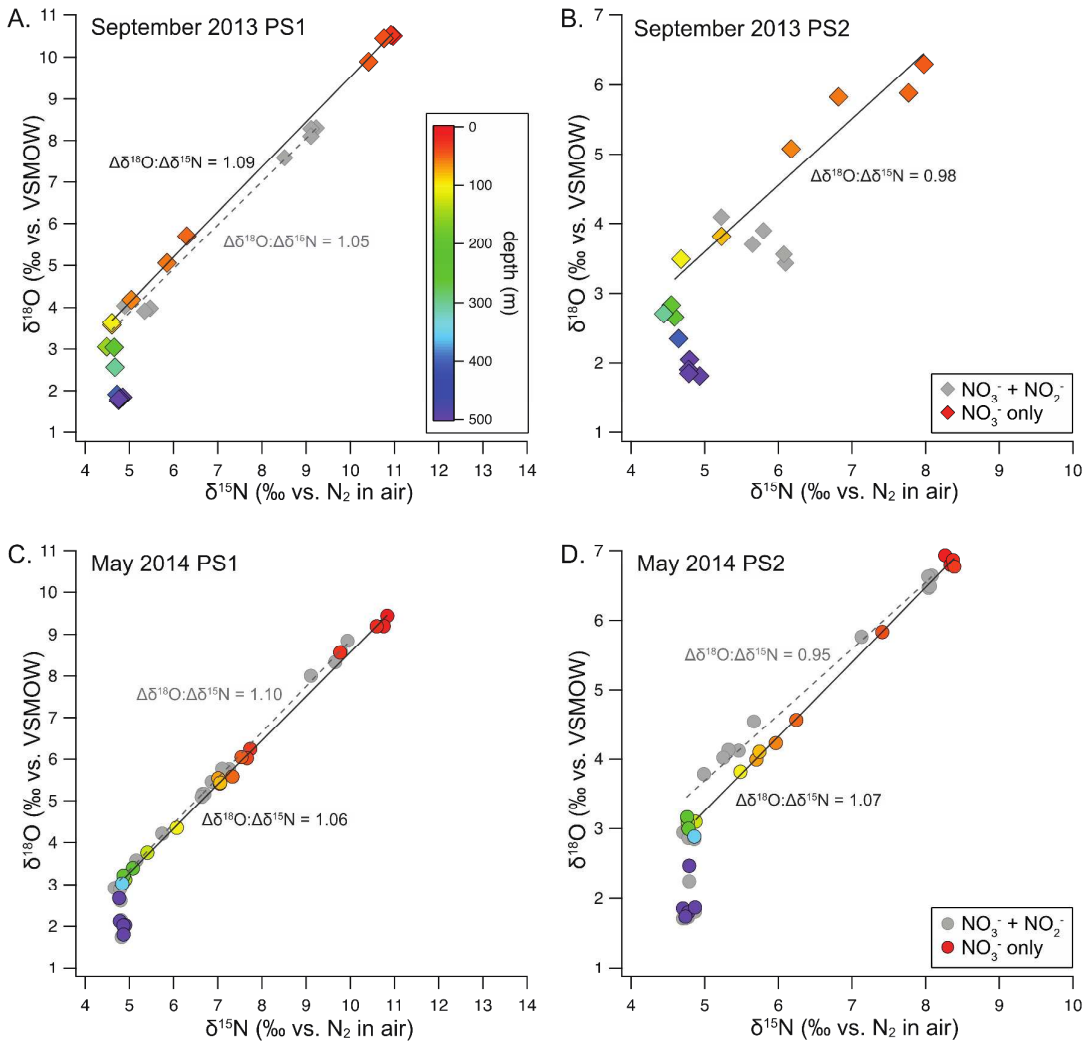

Figure 9:

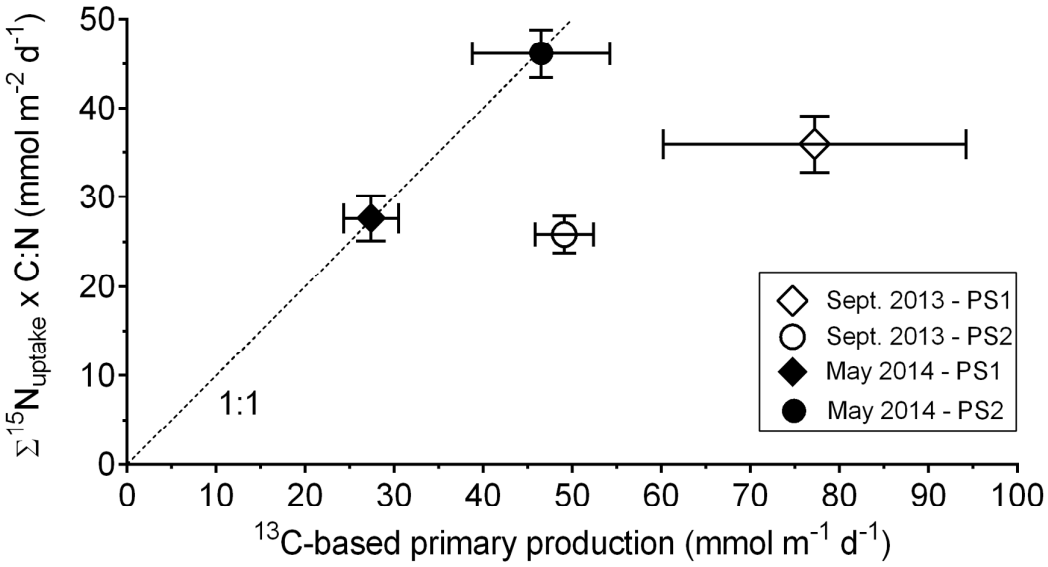

Supplemental Information for:

Nitrogen uptake and nitrification in the subarctic North Atlantic Ocean

Xuefeng Peng[1,2*], Sarah Fawcett[3*], Nicolas van Oostende[1], Martin Wolf[4], Dario Marconi[1], Daniel Sigman[1], and Bess Ward[1]

S1. Implications of the isotopic composition of nitrite for the origin of the primary nitrite maximum (PNM)

The $\delta^{15}N$ of nitrite (NO_2^-) may help to elucidate the origin of the PNM. In September, NO_2^- $\delta^{15}N$ calculated via mass balance ranged from -8.0 ± 3.3‰ to -2.7 ± 1.1‰, while in May, NO_2^- $\delta^{15}N$ was significantly lower ($P < 0.005$) at -31.6 ± 12.0‰ to -19.7 ± 8.6‰. Below, we compare these values with the $\delta^{15}N$ expected for NO_2^- deriving from phytoplankton efflux versus that resulting from an imbalance between NH_4^+ and NO_2^- oxidation.

We take the $\delta^{15}N$ of NO_3^- available to phytoplankton ($\delta^{15}N_{NO3external}$) to be that of the subsurface NO_2^- supply (4.8‰ at 150-250 m at all four stations), allowing for no prior uptake-driven $\delta^{15}N$ rise in order to yield the lowest (i.e., most conservative) estimate for the $\delta^{15}N$ of effluxed NO_2^-. The resultant $\delta^{15}N$ of NO_3^- inside a phytoplankton cell ($\delta^{15}N_{NO3internal}$) can be calculated by:

$$\delta^{15}N_{NO3internal} = \delta^{15}N_{NO3external} - {}^{15}\varepsilon_{NO3uptake} + (1-R)* {}^{15}\varepsilon_{NR} + R*{}^{15}\varepsilon_{NO3efflux} \quad \text{[Eqn. S1]}$$

where ${}^{15}\varepsilon_{NO3uptake}$ (2.0‰), ${}^{15}\varepsilon_{NR}$ (26.6‰), and ${}^{15}\varepsilon_{NO3efflux}$ (1.2‰) are the N isotope effects for NO_3^- uptake into the cell, reduction within the cell at the site of the NO_3^- reductase enzyme (NR), and efflux out of the cell (as per Karsh et al. 2012, 2014). R is the ratio of NO_3^- efflux relative to total NO_3^- uptake (Francois et al. 1993; Granger et al. 2010), estimated as:

$$R = ({}^{15}\varepsilon_{org} - {}^{15}\varepsilon_{NO3uptake})/({}^{15}\varepsilon_{NR} - {}^{15}\varepsilon_{NO3efflux}) \quad \text{[Eqn. S2]}$$

where ${}^{15}\varepsilon_{org}$ is the organism-level isotope effect (i.e., the net effect impart by an organism taking up NO_3^- on the $\delta^{15}N$ of seawater NO_3^-). From the NO_3^- isotope data, we estimate an average ${}^{15}\varepsilon_{org}$ of 3.1‰ in September and 5.2‰ in May (from the linear slope in NO_3^- $\delta^{15}N$ vs. $\ln([NO_3^-])$ (i.e., "Rayleigh" space). Given that culture and field data suggest ${}^{15}\varepsilon_{org}$ should be on the order of ~5‰ (Waser et al. 1998; Sigman et al. 1999; Needoba et al. 2003, 2004;

Needoba and Harrison 2004; Granger et al. 2010; Fawcett et al. 2015) and that a lower estimate is often indicative of upward mixing of subsurface NO_3^-, which violates the Rayleigh model (Sigman et al. 1999), we use the May estimate of 5.2‰ in our calculations. Substituting $^{15}\varepsilon_{org}$ into Eqn. S2 yields an estimate for R of 0.13, which in turn yields a $\delta^{15}N_{NO3internal}$ of 26.2‰. At steady state, the $\delta^{15}N$ of intracellular NO_2^- available for efflux into the water column will thus be -0.4‰ (i.e., 26.6‰ lower than $\delta^{15}N_{NO3internal}$).

The N isotope effect associated with NO_2^- efflux is unknown; if it is similar to $^{15}\varepsilon_{NO3efflux}$ (1.2‰; Karsh et al. 2014), then the $\delta^{15}N$ of effluxed NO_2^- could be as low as -1.6‰. We note that any isotopic fractionation associated with the intracellular reduction of NO_2^- will raise the $\delta^{15}N$ of the NO_2^- available for efflux. However, this seems improbable given that NO_2^- reduction occurs in the chloroplast, an organelle surrounded by at least three membranes across which NO_2^- would have to efflux. Moreover, the inhibition of NO_2^- transport into the chloroplast appears to be the controlling step preventing wasteful NO_3^- reduction to NH_4^+ (Rexach et al. 2000); this suggests that all NO_2^- transported into the chloroplast will be efficiently reduced, leaving no intra-chloroplast NO_2^- pool available for efflux. In any case, with a $\delta^{15}N \geq$-1.6‰, NO_2^- efflux by phytoplankton cannot account for the estimated $\delta^{15}N$ of NO_2^- in the upper 200 m in the subarctic North Atlantic (Figure 6). Moreover, if the lower values of $^{15}\varepsilon_{org}$ suggested by the nitrate isotope data are used for September, the $\delta^{15}N$ of effluxed NO_2^- could be as high as 1.1‰.

The concentration of NH_4^+ in open ocean surface waters is typically low, such that its $\delta^{15}N$ cannot be directly measured. We assume a $\delta^{15}N$ for NH_4^+ that is 3‰ lower than the average $\delta^{15}N$ of bulk PON in the euphotic zone (Altabet and Small 1990; Fawcett et al. 2011; Möbius 2013); this yields an NH_4^+ $\delta^{15}N$ of 1.3‰ to 2.7‰ in September and -2.2‰ to -2.0‰ in May (using a PON $\delta^{15}N$ of 4.3‰ to 5.7‰ for September and 0.8‰ to 1.0‰ for May). The NH_4^+ has two possible fates: uptake into the PON pool or oxidation to NO_2^-. If most of the NH_4^+ is taken up (for which, given the low NH_4^+ concentrations characteristic of the upper water column, we assume an isotope effect of 0‰; Hoch et al. 1992; Pennock et al. 1996; Vo et al. 2013; Liu et al. 2013) and only a small fraction is oxidized to NO_2^-, then the NH_4^+ oxidation isotope effect (estimated as 14‰-19‰ for marine nitrifiers; Casciotti et al. 2003) will be almost fully expressed, yielding NO_2^- with a $\delta^{15}N$ of -17.7‰ to -11.3‰ in September and -21.2‰ to -16.0‰ in May. By contrast, if most of the NH_4^+ is oxidized to NO_2^- and only a

small fraction is taken up, the NH_4^+ uptake isotope effect will be the primary driver of NO_2^- $\delta^{15}N$, yielding NO_2^- with a $\delta^{15}N$ very similar to the NH_4^+ from which it derived (i.e., 1.3‰ to 2.7‰ in September and -2.2‰ to -2.0‰ in May).

NO_2^- produced by NH_4^+ oxidation also has two possible fates: further oxidation to NO_3^- (with an isotope effect of -12.8‰; Casciotti 2009) or uptake into organic N (for which we assume an isotope effect of ~0‰, although very little information exists regarding this value; Waser et al., 1998). If most of the NO_2^- is taken up and only a small fraction is oxidized, the $\delta^{15}N$ of the NO_2^- not taken up will be virtually unchanged (i.e., -17.7‰ to -11.3‰ or 1.3‰ to 2.7‰ in September, and -21.2‰ to -16.0‰ or -2.2‰ to -2.0‰ in May). If, instead, most of the NO_2^- is oxidized, the oxidation isotope effect will be almost fully expressed, lowering the $\delta^{15}N$ of NO_2^- by as much as 12.8‰ (i.e., to -30.5‰ to -24.1‰ for NO_2^- with a starting $\delta^{15}N$ of -17.7‰ to -11.3‰ or to -11.5‰ to -10.1‰ for NO_2^- with an starting $\delta^{15}N$ of 1.3‰ to 2.7‰ in September; to -34.0‰ to -28.8‰ for NO_2^- with a starting $\delta^{15}N$ of -21.2‰ to -16.0‰ or to -15.0‰ to -14.8‰ for NO_2^- with an starting $\delta^{15}N$ of -2.2‰ to -2.0‰ in May).

It should be noted that the partial oxidation of NO_2^- deriving from phytoplankton efflux can decrease the $\delta^{15}N$ of the remaining NO_2^- pool by as much as -12.8‰ (Casciotti 2009). This means that while phytoplankton efflux may be the ultimate source of the NO_2^-, its isotopic composition can be lower than that calculated above for efflux; the lowest $\delta^{15}N$ that can achieved by this coupling is on the order of -14.4‰ for both September and May (i.e., -1.6‰ + (-12.8‰)).

While the results of this exercise are less conclusive for September than for May, they nonetheless suggest that the PNM derives mainly from NH_4^+ oxidation since this process can drive NO_2^- $\delta^{15}N$ to the very low $\delta^{15}N$ values observed (Figure 6B).

S2. Calculation of nitrogen and carbon uptake rates

The rates of NH_4^+ and NO_3^- uptake (ρ_{NH4} and ρ_{NO3}, respectively) were calculated as:

$$\rho_N = \frac{R_{PON(t)} - R_{PON(0)}}{(R_{DIN(0)} - R_{PON(0)}) \times \Delta t} \times [PON]_{(t)} \quad \text{[Eqn S3]}$$

where:

ρ_N is the N uptake rate (nmol l^{-1} hr^{-1})

$R_{PON(t)}$ is the measured ratio of $^{15}N/^{14}N$ in the particulate organic nitrogen (PON) pool at the end of the incubation

$R_{PON(0)}$ is the initial $^{15}N/^{14}N$ of the PON pool, calculated using the measured water column $\delta^{15}N$ of PON at this site according to:

$$R_{PON(0)} = R_{air} \times \left(1 + \frac{\delta^{15}N_{ambient}}{1000}\right) \quad \text{[Eqn S4]}$$

$R_{DIN(0)}$ is the initial ratio of $^{15}N/^{14}N$ in the dissolved inorganic nitrogen (DIN) pool, and is calculated from the measured ambient concentration of NH_4^+ or NO_3^- ($[N]_{ambient}$), the $\delta^{15}N$ of NH_4^+ or NO_3^- ($\delta^{15}N_{DINambient}$, where the $\delta^{15}N$ of NO_3^- was measured using the denitrifier-IRMS method (Sigman et al. 2001)) and the $\delta^{15}N$ of NH_4^+ was assumed to be 3‰ lower than the measured $\delta^{15}N$ of PON (Altabet and Small 1990; Fawcett et al. 2011; Möbius 2013); and the concentration ($[N]_{tracer}$) and $^{15}N/^{14}N$ (R_{tracer}; 0.99) of the tracer addition according to:

$$R_{DIN(0)} = \frac{[N]_{ambient} \times R_{air} \times (1 + \delta^{15}N_{DINambient}/1000) + [N]_{tracer} \times R_{tracer}}{[N]_{ambient} + [N]_{tracer}} \quad \text{[Eqn S5]}$$

Δt is the duration of incubation (hr)

$[PON]_{(t)}$ is the measured PON concentration at the end of incubation (nmol l^{-1}).

ρ_{NH4} and ρ_{NO3} were converted to per day rates (i.e., nmol l^{-1} d^{-1}) assuming uptake occurred during the 12 hours of daylight.

Finally, at each depth, the f-ratio was calculated according to Eppley and Peterson (1979) as:

$$f = V_{new}/(V_{new} + V_{regenerated}) \quad \text{[Eqn S6]}$$

where V_{new} is calculated as $\rho_{NO3}/[PON]_{(t)}$ and $V_{regenerated}$ is $\rho_{NH4}/[PON]_{(t)}$. Below, we report and discuss only the euphotic zone average f-ratios for each station, calculated by trapezoidally integrating the f-ratios measured at each depth and then dividing by the depth of the euphotic zone (i.e., a weighted average).

The duration of the experiments (~7-9 hours, beginning at dawn) means that the resultant carbon fixation rates best approximate net primary production (NPP) (Cullen 2001). The hourly rate of photosynthetic carbon fixation by the phytoplankton community was determined from duplicate incubation samples by normalising the rate of dissolved inorganic carbon (DIC) incorporation into POC to the length of the incubation, calculated following (Legendre and Gosselin 1997).

which was calculated as:

$$\rho_C = \frac{R_{POC(t)} - R_{POC(0)}}{(R_{DIC(0)} - R_{POC(0)}) \times \Delta t} \times [POC]_{(t)} \qquad \text{[Eqn S7]}$$

where:

ρ_C is the rate of NPP (nmol l^{-1} h^{-1});

$R_{POC(t)}$ is the measured ratio of $^{13}C/^{12}C$ in the particulate organic carbon (POC) pool at the end of the incubation;

$R_{POC(0)}$ is the initial $^{13}C/^{12}C$ of the POC pool, assumed to be natural abundance (i.e., 0.011);

Δt is the duration of incubation (day);

$[POC]_{(t)}$ is the measured POC concentration at the end of incubation (nmol l^{-1});

and $R_{DIC(0)}$ is the initial ratio of $^{13}C/^{12}C$ in the DIC pool, calculated as:

$$R_{DIC(0)} = \frac{[DIC]_{ambient} \times R_{ambient} + [DIC]_{tracer} \times R_{tracer}}{[DIC]_{ambient} + [DIC]_{tracer}} \qquad \text{[Eqn S8]}$$

where:

$[DIC]_{ambient}$ is taken to be 2.1 x 10^6 nmol l^{-1} (Zunino et al. 2015);

$R_{ambient}$ is the $^{13}C/^{12}C$ of the ambient DIC pool, taken to be natural abundance (i.e., 0.011);

$[DIC]_{tracer}$ is the concentration of $NaH^{13}CO_3$ added to the incubation bottles (nmol l^{-1});

and R_{tracer} is the $^{13}C/^{12}C$ of the added tracer (i.e., 0.85). ρ_C was converted to per day rates (i.e., nmol l^{-1} d^{-1}) assuming uptake occured during the 12 hours of daylight.

Figure S1: The positive correlation between particular nitrogen (PON_{integ}) and the sum of NH_4^+ and NO_3^- uptake rates integrated over the euphotic zone at the four stations sampled in this study.

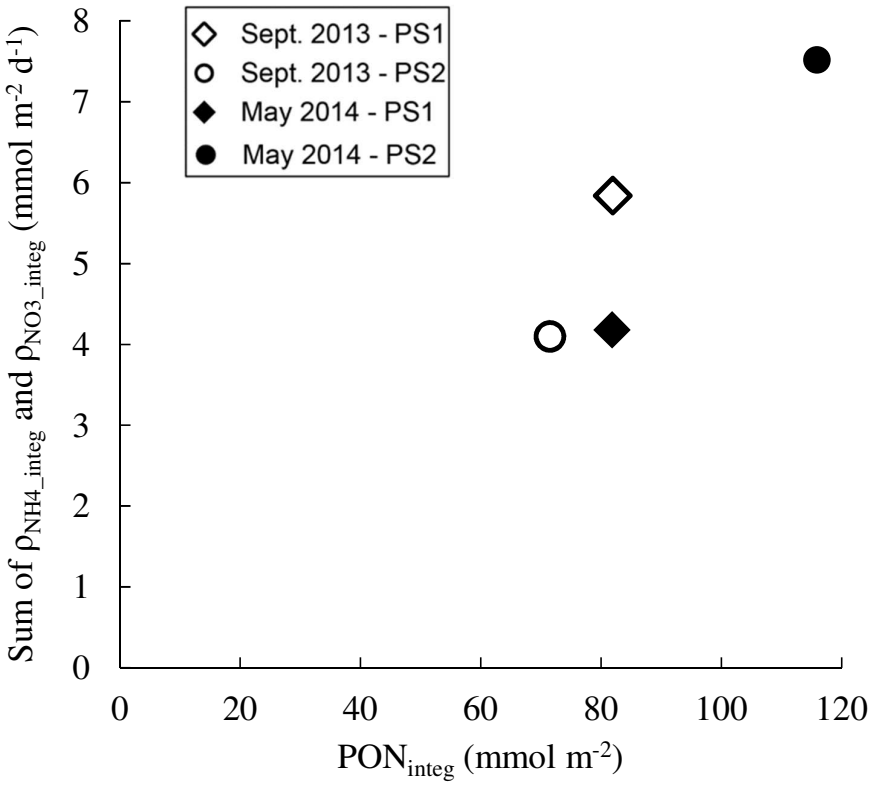

References

Altabet, M. A., and L. F. Small. 1990. Nitrogen isotopic ratios in fecal pellets produced by marine Zooplankton. Geochim. Cosmochim. Acta **54**: 155–163. doi:10.1016/0016-7037(90)90203-W

Casciotti, K. L. 2009. Inverse kinetic isotope fractionation during bacterial nitrite oxidation. Geochim. Cosmochim. Acta **73**: 2061–2076. doi:10.1016/j.gca.2008.12.022

Casciotti, K. L., D. M. Sigman, and B. B. Ward. 2003. Linking Diversity and Stable Isotope Fractionation in Ammonia-Oxidizing Bacteria. Geomicrobiol. J. **20**: 335–353. doi:10.1080/01490450303895

Cullen, J. J. 2001. Primary production methods. Mar. Ecol. Prog. Ser. **52**: 2277–2284.

Eppley, R. W., and B. J. Peterson. 1979. Particulate organic matter flux and planktonic new production in the deep ocean. Nature **282**: 677–680. doi:10.1038/282677a0

Fawcett, S. E., M. W. Lomas, J. R. Casey, B. B. Ward, and D. M. Sigman. 2011. Assimilation of upwelled nitrate by small eukaryotes in the Sargasso Sea. Nat. Geosci. **4**: 717–722. doi:10.1038/ngeo1265

Fawcett, S. E., B. B. Ward, M. W. Lomas, and D. M. Sigman. 2015. Vertical decoupling of nitrate assimilation and nitrification in the Sargasso Sea. Deep-Sea Res. Part I: 64–72. doi:10.1016/j.dsr.2015.05.004

Francois, R., M. P. Bacon, M. A. Altabet, and L. D. Labeyrie. 1993. Glacial/interglacial changes in sediment rain rate in the SW Indian Sector of subantarctic Waters as recorded by 230Th, 231Pa, U, and δ15N. Paleoceanography **8**: 611–629. doi:10.1029/93PA00784

Granger, J., D. M. Sigman, M. M. Rohde, M. T. Maldonado, and P. D. Tortell. 2010. N and O isotope effects during nitrate assimilation by unicellular prokaryotic and eukaryotic plankton cultures. Geochim. Cosmochim. Acta **74**: 1030–1040.

Hoch, M. P., M. L. Fogel, and D. L. Kirchman. 1992. Isotope fractionation associated with ammonium uptake by a marine bacterium. Limnol. Oceanogr. **37**: 1447–1459. doi:10.4319/lo.1992.37.7.1447

Karsh, K. L., J. Granger, K. Kritee, and D. M. Sigman. 2012. Eukaryotic Assimilatory Nitrate Reductase Fractionates N and O Isotopes with a Ratio near Unity. Environ. Sci. Technol. **46**: 5727–5735. doi:10.1021/es204593q

Karsh, K. L., T. W. Trull, D. M. Sigman, P. A. Thompson, and J. Granger. 2014. The contributions of nitrate uptake and efflux to isotope fractionation during algal nitrate assimilation. Geochim. Cosmochim. Acta **132**: 391–412. doi:10.1016/j.gca.2013.09.030

Legendre, L., and M. Gosselin. 1997. Estimation of N or C uptake rates by phytoplankton using 15N or 13C: revisiting the usual computation formulae. J. Plankton Res. **19**: 263–271. doi:10.1093/plankt/19.2.263

Liu, K.-K., S.-J. Kao, K.-P. Chiang, G.-C. Gong, J. Chang, J.-S. Cheng, and C.-Y. Lan. 2013. Concentration dependent nitrogen isotope fractionation during ammonium uptake by phytoplankton under an algal bloom condition in the Danshuei estuary, northern Taiwan. Mar. Chem. **157**: 242–252. doi:10.1016/j.marchem.2013.10.005

Möbius, J. 2013. Isotope fractionation during nitrogen remineralization (ammonification): Implications for nitrogen isotope biogeochemistry. Geochim. Cosmochim. Acta **105**: 422–432. doi:10.1016/j.gca.2012.11.048

Needoba, J. A., and P. J. Harrison. 2004. Influence of Low Light and a Light: Dark Cycle on No3– Uptake, Intracellular No3–, and Nitrogen Isotope Fractionation by Marine Phytoplankton1. J. Phycol. **40**: 505–516. doi:10.1111/j.1529-8817.2004.03171.x

Needoba, J. A., D. M. Sigman, and P. J. Harrison. 2004. The Mechanism of Isotope Fractionation During Algal Nitrate Assimilation as Illuminated by the 15n/14n of Intracellular Nitrate1. J. Phycol. **40**: 517–522. doi:10.1111/j.1529-8817.2004.03172.x

Needoba, J. A., N. A. Waser, P. J. Harrison, and S. E. Calvert. 2003. Nitrogen isotope fractionation in 12 species of marine phytoplankton during growth on nitrate. Mar. Ecol. Prog. Ser. **255**: 81–91. doi:10.3354/meps255081

Pennock, J. R., D. J. Velinsky, J. M. Ludlam, J. H. Sharp, and M. L. Fogel. 1996. Isotopic fractionation of ammonium and nitrate during uptake by Skeletonema costatum: Implications for δ15N dynamics under bloom conditions. Limnol. Oceanogr. **41**: 451–459. doi:10.4319/lo.1996.41.3.0451

Rexach, J., E. Fernández, and A. Galván. 2000. The Chlamydomonas reinhardtii Nar1 Gene Encodes a Chloroplast Membrane Protein Involved in Nitrite Transport. Plant Cell **12**: 1441–1453. doi:10.1105/tpc.12.8.1441

Sigman, D. M., M. A. Altabet, D. C. McCorkle, R. Francois, and G. Fischer. 1999. The δ15N of nitrate in the southern ocean: Consumption of nitrate in surface waters. Glob. Biogeochem. Cycles **13**: 1149–1166. doi:10.1029/1999GB900038

Sigman, D. M., K. L. Casciotti, M. Andreani, C. Barford, M. Galanter, and J. K. Böhlke. 2001. A Bacterial Method for the Nitrogen Isotopic Analysis of Nitrate in Seawater and Freshwater. Anal. Chem. **73**: 4145–4153. doi:10.1021/ac010088e

Vo, J., W. Inwood, J. M. Hayes, and S. Kustu. 2013. Mechanism for nitrogen isotope fractionation during ammonium assimilation by Escherichia coli K12. Proc. Natl. Acad. Sci. **110**: 8696–8701. doi:10.1073/pnas.1216683110

Waser, N. a. D., P. J. Harrison, B. Nielsen, S. E. Calvert, and D. H. Turpin. 1998. Nitrogen isotope fractionation during the uptake and assimilation of nitrate, nitrite, ammonium, and urea by a marine diatom. Limnol. Oceanogr. **43**: 215–224. doi:10.4319/lo.1998.43.2.0215

Zunino, P., P. Lherminier, H. Mercier, X. A. Padín, A. F. Ríos, and F. F. Pérez. 2015. Dissolved inorganic carbon budgets in the eastern subpolar North Atlantic in the 2000s from in situ data. Geophys. Res. Lett. **42**: 2015GL066243. doi:10.1002/2015GL066243